TNO innovation for life

Technical Sciences
Van Mourik Broekmanweg 6
2628 XE Delft
P.O. Box 49
2600 AA Delft
The Netherlands

www.tno.nl

T +31 88 866 30 00
F +31 88 866 30 10

TNO report

TNO 2016 R10421

Monitoring Network Building Vibrations - Analysis Earthquake 30-09-2015 (Hellum)

Date	March 29, 2016
Author(s)	██████████ ████████████████
Copy no	2016.0100295515
No. of copies	
Number of pages	65 (incl. appendices)
Number of appendices	
Sponsor	NAM PO Box 28000 9400 HH Assen
Project name	Earthquake Hellum
Project number	060.16792/01.12

Contents

H Registration form for repetitive damage survey
I   Results repetitive damage survey

1 Introduction

1.1 Background

In Groningen, so-called induced earthquakes occur, as a result of the extraction of natural gas. These earthquakes cause ground-borne vibrations that transfer to the foundations of buildings thus causing the building itself to vibrate. These vibrations may result in damage to the building.

To determine the effects of the induced earthquakes, NAM has set up a research program. Part of this research program is a monitoring network for building vibrations. In about 200 buildings a vibration sensor is installed, measuring continuously the building vibrations at foundation level. To gain insight in the vulnerability of the buildings in Groningen for particular vibration levels, this monitoring network also includes a damage survey. By surveying the damage in these buildings before and after an earthquake, a relation can be found between the building vibrations due to an earthquake and the damage in the buildings caused by that earthquake.

TNO has designed and built this monitoring network for building vibrations, including an IT infrastructure to handle, process and analyse the data (the vibration data centre). The set-up of this monitoring network is described in TNO-report 2015 R10501 "Monitoring Network Building Vibrations" [ref 01].

1.2 Purpose

On September 30th 2015, an earthquakes took place at Hellum. According to the website of KNMI the characteristics of this earthquakes are:

- Name: Hellum
- Date: 30th September 2015
- Time: 18:05h (UTC)
- Magnitude: M = 3.1
- Location epicentre (latitude/longitude): 53234 / 6834
- Location epicentre (X-Y): 251603 / 584016

NAM has commissioned TNO to analyse the effects of this earthquake on the buildings of the monitoring network. These analyses comprise the transfer of ground-borne vibrations to building vibrations and the damage inflicted on the buildings due to the earthquake vibration.

1.3 Guide

This report describes the results of the analysis of the earthquake.
Firstly, Chapter 2 provides a general description of the set-up of the monitoring network building vibrations. Subsequently, Chapter 3 gives an overview of the buildings for which the measured vibration velocity at foundation level has exceeded a preset trigger value.

The analysis of the building vibrations is given in Chapter 4 – 6. Chapter 4 describes the framework of this analysis, Chapter 5 presents an analysis of the building vibrations and Chapter 6 presents an analysis of the transfer of the ground borne vibrations to the building vibrations.

The analysis of the building damage, caused by the earthquake, is given in Chapter 7 – 9. Chapter 7 describes the framework of this analysis, Chapter 8 gives the results of the repetitive damage surveys and Chapter 9 the damage curves.

Finally, Chapter 10 to 12 give the conclusions, references and the signature.

1.4 Former reports

This report is a third report of the Monitoring Network Building Vibrations with an analysis of the effects of the earthquakes. The former reports were:
- TNO report 2015R10604 "Monitoring Network Building Vibrations – Analysis Earthquake 30-09-2014 Garmerwolde" [ref 04].
- TNO report 2015R10604 "Monitoring Network Building Vibrations – Analysis Earthquakes 05-11-2014 (Zandeweer), 30-12-2014 (Woudbloem) and 06-01-2015 (Wirdum)" [ref 05].

2   Set-up of the analysis procedures of the monitoring network

The analysis procedure of the monitoring network is based on the path the vibrations travel from source to building. The path the vibrations travel comprises of (Figure 2.1):

1.   Ground-borne vibrations caused by an earthquake which spread towards the surroundings.
2.   Ground-borne vibrations which are transferred to the buildings and result in vibration loads on the building foundations.
3.   Building vibrations which can cause damage.

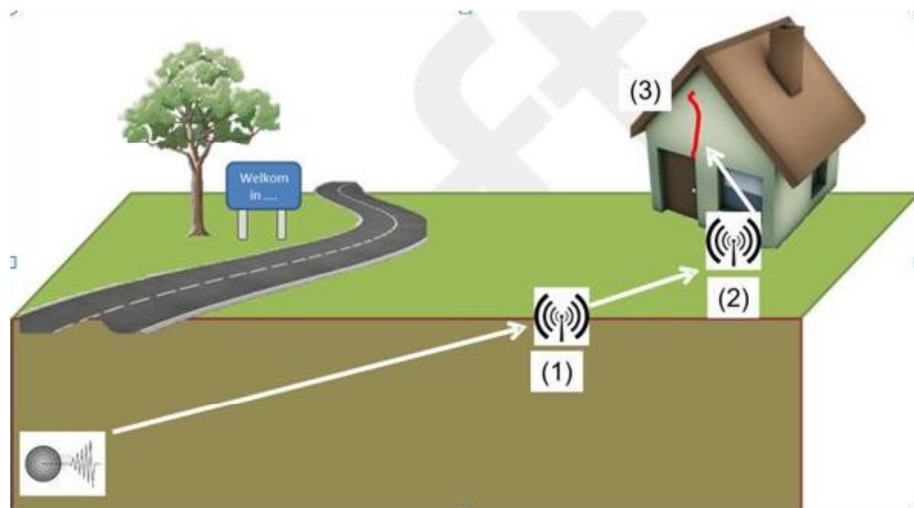The effects caused in the three steps are analysed separately.

Figure 2.1: Illustration of the vibration path of an earthquake

Ad 1: Ground-borne vibrations
The ground-borne vibrations of step 1 are measured and analysed by KNMI via their own (separate) monitoring network, hence this effect is not part of the analysis procedure of this monitoring network. However, the ground-borne vibrations measured by KNMI do provide valuable input for step 2 and some data of the KNMI monitoring network is therefore included in the analysis.

Ad 2: Vibration load on buildings
Ground-borne vibrations are (probably) not transferred to the buildings one-to-one. The extent to which the ground-borne vibrations are transferred to buildings is characterised in practice by a transfer function. The transfer of vibrations depends on several factors, such as local soil conditions, type of foundation, etc.
To obtain insight into the transfer of the vibrations, vibration measurements are performed in about 200 buildings, at foundation level. Those measurements are then linked to the ground-borne vibrations measured or calculated by the KNMI in order to determine the transfer functions.
The buildings included in the monitoring network are selected such that they are representative for the majority of the buildings in Groningen.

<u>Ad 3: Damage caused by vibrations</u>
In the Netherlands there are no regulations for the determination of damage due to vibration loads on buildings. To ascertain the probability of building damage as a result of vibrations the SRB guideline A [02] provides damage curves. These damage curves show the relationship between the building vibration velocity and the probability of damage, for masonry in good and poor condition and for monuments, based on practical experience.

Although these damage curves can be used to establish the probability of damage for a particular vibration velocity, they provide no information on the severity of the damage.

After each earthquake above a magnitude M=2.5 a damage survey is carried out in the buildings that have a vibration level above a pre-set threshold (v=1 mm/s). The severity of the damage is classified in damage categories. By plotting the damage categories of the respective buildings against the vibration characteristics, new damage curves can be established in which the severity of the damage is related to the vibration characteristics on foundation level.

3 Buildings triggered by earthquakes

The buildings for which the measured foundation vibration velocity (v_{max}) has exceeded 1 mm/s are analysed (see TNO-report "Monitoring Network Building Vibrations" [01]). This trigger level of 1 mm/s is commonly regarded as the lower limit for damage due to vibrations.

During the Hellum earthquake, the building vibration velocity at foundation level (v_{max}) exceeded 1 mm/s in a total of 40 buildings:
- 38 triggered buildings are houses; these are selected for both signal analysis and damage analysis.
- 2 triggered buildings are town halls (████) and (████); these are selected for signal analysis, but excluded from damage analysis.
- For 1 triggered house (████) an event file (extensive vibration signal during earthquake) was not generated, because the trigger was just at the trigger level of 1 mm/s. Therefore only a damage analysis is included and not a signal analysis.
- For 2 houses vibration data was not available, due to out of order of the measuring equipment (████) and (████). However, based on the vibration data of nearby houses, it is expected that the vibration level in these two houses has exceeded the trigger level. Therefore these two houses are also selected for damage analysis.

An overview of the triggered buildings is given in table 3.1. This table provides the following information:
- Building ID number
- Building type (see Annex A; Table A.1)
- Year of construction
- Foundation type
- Damage state (DS) at the most recent damage survey before the earthquake
- Maximum measured, horizontal component of the building vibration velocity at foundation level ($v_{x,y,max}$) during the earthquake (for definition $v_{x,y,max}$ see Paragraph 4.2).
- The data the last damage survey and the repetitive damage survey took place.

Additionally Figure 3.1 shows the maximum measured, horizontal component of the building vibration velocities at foundation level ($v_{x,y,max}$) of all buildings with respect to the epicentre of the earthquake as given by KNMI (see Chapter 1.2).

Table 3.1: Buildings triggered by Hellum earthquake

| ID	Type	Year of construction	Foundation type	Damage state (DS; before earthquake)	$v_{x,y,max}$ (mm/s)	Damage survey	
						Last survey	Survey Hellum
■	6	1929	no piles	2	2.6	14-7-2014	29-10-2015
■	9	1995	no piles	1	5.2	20-2-2015	22-10-2015
■	4	1905	no piles	1	1.0	10-2-2015	21-10-2015
■	3	1987	no piles	1	5.0	28-7-2014	19-10-2015
■	9	1998	no piles	1	3.2	16-7-2014	19-10-2015
■	4	1930	no piles	1	1.1	15-6-2015	22-10-2015
■	9	1994	no piles	1	6.8	18-7-2014	--**
■	9	1998	no piles	2	11.1	1-8-2014	26-10-2015
■	9	1994	no piles	1	6.9	18-7-2014	20-10-2015
■	9	1976	no piles	1	1.6	8-5-2015	30-11-2015
■	7	1953	no piles	2	5.2	11-5-2015	26-10-2015
■	5	1930	no piles	2	5.3	19-9-2014	20-10-2015
■	8	1975	unknown	1	2.0	12-5-2015	20-10-2015
■	7	1963	no piles	2	1.5	28-8-2014	20-10-2015
■	9	1987	no piles	1	6.7	28-7-2014	29-10-2015
■	3	2006	no piles	1	6.2	30-4-2015	20-10-2015
■	5	1920	unknown	2	--	8-12-2014	30-9-2015
■	7	1950	no piles	1	7.6	21-7-2014	19-10-2015
■	8	2010	piles	1	1.1	29-1-2015	21-10-2015
■	8	2001	piles	1	1.6	31-7-2014	20-10-2015
■	9	1978	no piles	1	1.7	16-9-2014	20-10-2015
■	8	1990	piles	1	2.0	2-6-2015	--**
■	9	1996	no piles	1	1.5	20-2-2015	22-10-2015
■	1	1980	no piles	1	--	20-2-2015	21-10-2015
■	2	1980	no piles	1	5.1	20-2-2015	20-10-2015
■	1	1968	unknown	1	5.3	9-9-2014	19-10-2015
■	2	1968	unknown	1	5.3	10-9-2014	19-10-2015
■	1	1971	piles	1	1.2	28-1-2015	22-10-2015
■	2	1971	piles	1	1.1	28-1-2015	22-10-2015
■	7	1959	no piles	1	1.6	18-5-2015	22-10-2015
■	4	1940	unknown	2	1.9	19-5-2015	26-10-2015
■	2	1973	no piles	0	1.0	20-5-2015	21-10-2015
■	7	1956	piles	2	2.0	21-5-2015	21-10-2015
■	3	1997	piles	1	1.5	3-6-2015	20-10-2015
■	6	1900	no piles	1	4.5	10-6-2015	23-10-2015
■	3	1936	no piles	1	1.3	28-5-2015	26-10-2015
■	9	1993	no piles	1	1.6	20-5-2015	20-10-2015
■	7	1959	no piles	1	1.2	22-5-2015	21-10-2015
■	5	1888	unknown	2	1.0	5-6-2015	21-10-2015
■	8	2008	piles	1	1.1	25-9-2015	23-10-2015
■*	0	--	--	--	1.0	--	--
■*	0	--	--	--	10.3	--	--

* = town hall

** = see Chapter 8
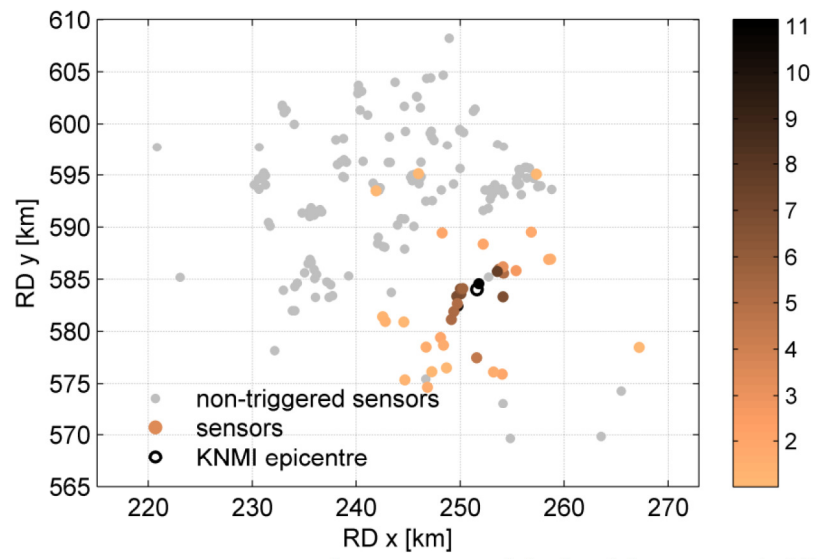
Figure 3.1: Overview of the maximum measured, horizontal component of the building vibration velocity at foundation level ($v_{x,y,max}$ mm/s) with respect to the epicentre of the Hellum earthquake

4 Framework analysis building vibrations

4.1 General

The building sensors measure building vibration accelerations at foundation level. Out of these measured accelerations the sensor systems calculate directly the vibration velocity and these calculated vibration velocities are used to determine if the pre set trigger, a vibration velocity of 1 mm/s, is exceeded.
After the pre set trigger is exceeded, the sensor system sends the originally measured vibration accelerations to the vibration data center (VDC). These originally measured accelerations are used for the analysis of the building vibrations.

4.2 Vibration characteristics

For each building the measured acceleration signal by the building sensor is analysed as follows (Figure 4.1):
- Two time-domain signals are calculated:
  - The raw measured acceleration signal a(t) is used after removal of the offset.
  - After filtering the signal is integrated to a velocity signal v(t).
- The frequency spectrum is calculated for the acceleration and the velocity signals.
- Individual signal characteristics are calculated for each of the three signal directions per sensor (two in horizontal direction (x and y) and one in vertical direction (z)):
  - Acceleration [a]; this value is used in international earthquake guidelines and is of interest for structural calculations. Calculated values are: $a_{x, max}$, $a_{y, max}$, $a_{z, max}$ and $a_{x,y,max}$ (=peak acceleration in horizontal direction).
  - Velocity [v]; this value is used in the Dutch guidelines (SBR ref [02]) for relations between building vibrations and the probability of damage. Calculated values are: $v_{x, max}$, $v_{y, max}$, $v_{z, max}$ and $v_{x,y,max}$ (=peak velocity in horizontal direction).
  - Effective velocity [$v_{eff,max}$]; this value is mostly used to express a relation between the vibration and the hindrance for people (ref [03]).
  - Dominant frequency of acceleration [$f_{a,dom}$] and velocity [$f_{v,dom}$]; these values are of interest for the transfer of the ground-borne vibrations to the building vibrations.
  - The vectorial maximum of the acceleration ($|a(t)|_{max}$) and the velocity ($|v(t)|_{max}$) are calculated ($|a(t)| = \sqrt{(a_x(t))^2 + (a_y(t))^2 + (a_z(t))^2}$). These are absolute values of the acceleration and the velocity, independent from the orientation of the sensor.
  - The Arias Intensity. For the x-channel this is given by $I_{A,x} = \frac{\pi}{2g} \int_0^T a_x(t)^2 dt$ with T the length of the time trace. The y- and z-channels are calculated in a similar way.
  - The Total Arias Intensity. This is given by $I_{A,total} = I_{A,x} + I_{A,y} + I_{A,y}$.
  - The Cumulative Absolute Velocity (CAV). For the x-channel this is given by: $CAV_x = \int_0^T |a_x(t)| dt$ and similar for the y- and z- channels.
  - The Total Cumulative Absolute Velocity. This is given by $CAV_{total} = CAV_x + CAV_y + CAV_z$.

- The Standardized Cumulative Absolute Velocity CAV$_{STD}$. This is calculated in a similar fashion as the CAV but here the signal is divided into 1 second long sections and a section is only taken into account if there is a moment in the section where the absolute acceleration is above a certain threshold. Currently this threshold is set to 0.001g. This prevents the CAV$_{STD}$ from keeping accumulating after the event contrary to the CAV can do.

The calculation of the Arias Intensity, CAV and CAVSTD is performed on the raw acceleration signal after offset removal. No filtering is applied. Tests show that results differ less than 1% for the current events. Larger events are likely to have a lower frequency content which is perhaps partly affected by the filter, so it has been chosen to perform the calculations on the unfiltered signal.
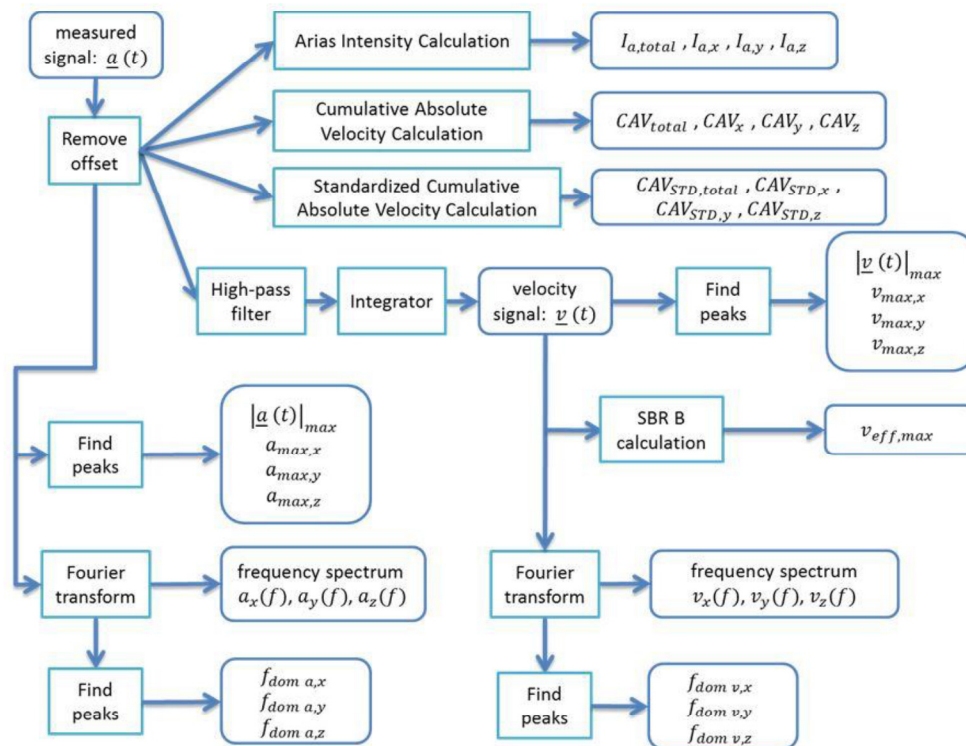

Figure 4.1: Flow chart for analysing signal characteristics

4.3   Transfer functions

There are three main sources of information along the chain from the epicenter of an earthquake to the exposed buildings, namely:
  (i)   the magnitude and location of the earthquake
  (ii)   the free-field signal characteristics at the KNMI instrument points
  (iii)   the foundation signal characteristics in the buildings.
The first two sources are covered by KNMI. KNMI has installed free-field sensors in a grid of 6 km within the area of the monitoring network, to measure the free field characteristics. The relationship between the vibration signal characteristics at the KNMI free-field points (ii) and the ones measured on the building foundations (iii) will be calculated as part of the monitoring network building vibrations.

 For each building, the KNMI free-field data at the KNMI point closest to the building and the measured foundation signals will be used to calculate the transfer function of the ground-borne vibrations to the building vibrations at foundation level.

For each building triggered the closest by KNMI free-field sensor has been selected. The signal from this free-field sensor has been analyzed in the same way as the signal from the building sensors (see Chapter 4.2).
Since the horizontal vibration components of the free-field sensors are given in the direction of the epicenter and perpendicular to that direction, these values cannot be compared to the horizontal components of the building sensors directly. The horizontal components of the free-field sensors have to be rotated to the x- and y-direction of the individual buildings.

The transfer of ground-borne vibrations to building vibrations will be determined for each of the individual signal characteristics, as a transfer factor: ratio between the comparable single-figures. This will be done for all three measuring directions.
As an example, the transfer factor for the peak velocity can be determined as follows:

- Peak ground velocity in three directions (i=1,2,3): $v_{max,ground\ borne,i}$
- Peak foundation velocity in three directions (i=1,2,3): $v_{max,building,i}$
- Transfer factor in three directions (i=1,2,3): T_i

$$T_{v_{max},i} = \frac{v_{max,foundation,i}}{v_{max,ground-borne,i}}$$

NOTE:
At the moment this Paragraph was written the sensor network of KNMI was not yet finished and no sufficient data was available. It is possible that the final way in which the data will be provided to TNO will lead to some adjustments to the above mentioned analysis.

5 Vibration characteristics

The vibration signals of the triggered buildings are recorded for a period of 30 s, about 10 s before and 20 s after the beginning of the signal from the earthquake. An example of such a vibration signal is given in Figure 5.1. Annex B of this report gives examples of the measured vibration acceleration signals of four buildings for the Hellum earthquake. The same Annex also gives graphs with the distribution of the frequency of each signal.
Annex C gives the same information regarding the calculated vibration velocity signals and the distribution of the frequency of each signal.
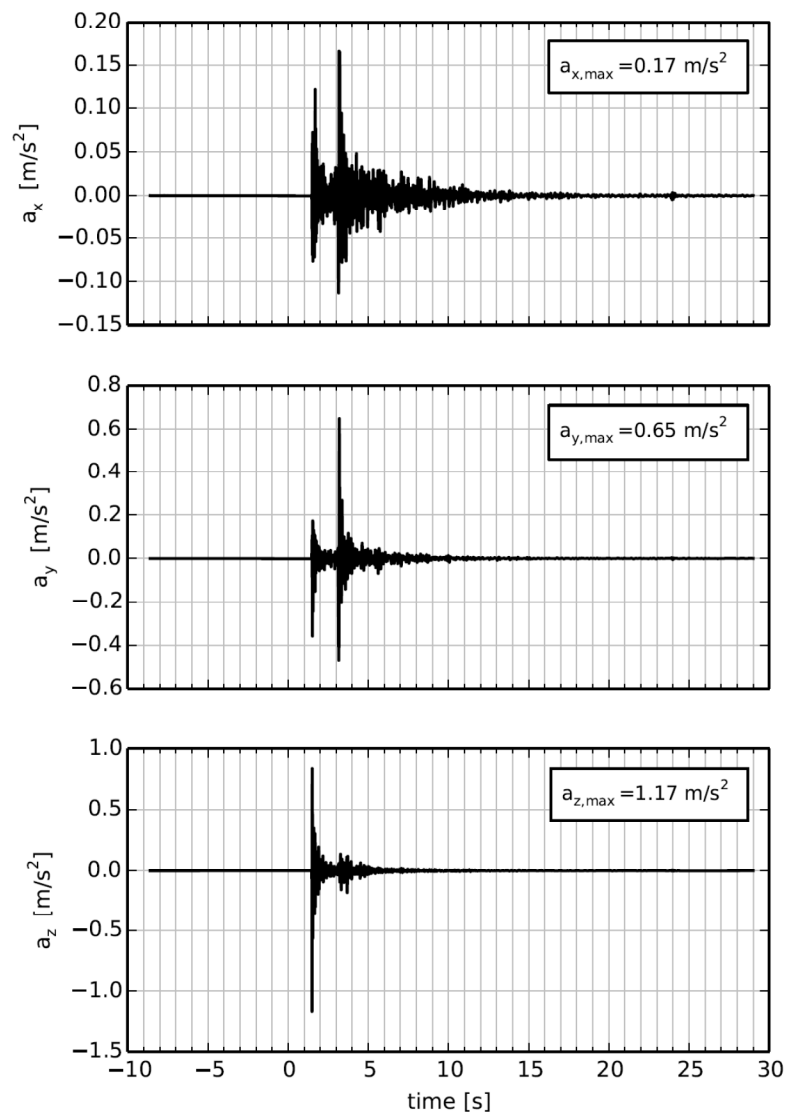

Figure 5.1: Example of a measured vibration acceleration signal from the Hellum event (ID ▇▇).

The calculated vibration characteristics regarding the acceleration are given in Annex D:

- Peak acceleration in three directions: $a_{x,max}$, $a_{y,max}$, $a_{z,max}$
- Peak acceleration in horizontal direction: $a_{x,y,max}$ = maximum ($a_{x,max}$ and $a_{y,max}$)
- Vectorial maximum of the acceleration: maximum of $|a(t)|$
- Dominant frequency of acceleration in three directions: $f_{a,dom,x}$, $f_{a,dom,y}$, $f_{a,dom,z}$

The peak vibration acceleration of all buildings triggered by the Hellum earthquake is presented in Figure 5.2. A distinction is made between the horizontal (x,y) and the vertical (z) component of the vibration acceleration.
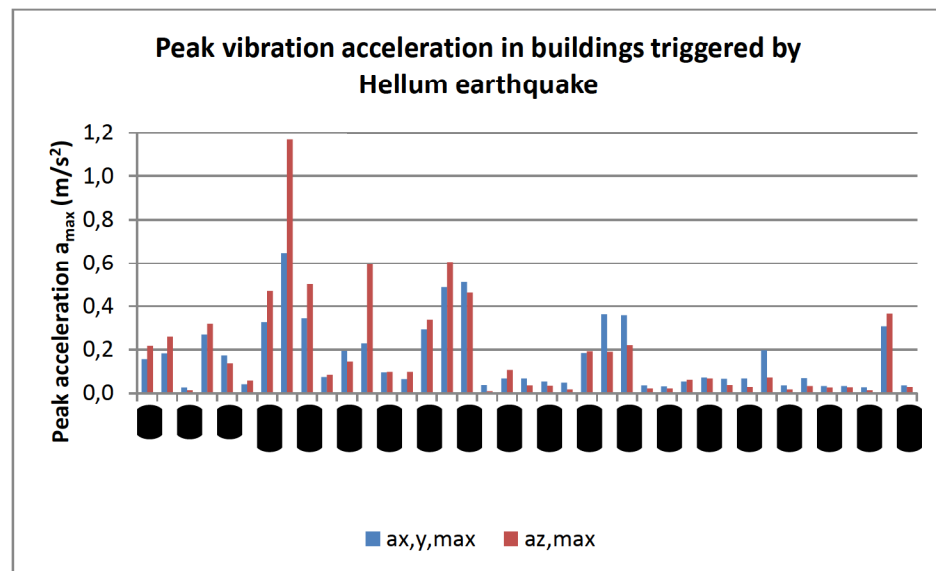

Figure 5.2: Peak acceleration of all buildings triggered by the Hellum earthquake

The calculated vibration characteristics regarding the velocity are given in Annex E:

- Peak velocity in three directions: $v_{x,max}$, $v_{y,max}$, $v_{z,max}$
- Peak velocity in horizontal direction: $v_{x,y,max}$ = maximum ($v_{x,max}$ and $v_{y,max}$)
- Vectorial maximum of the velocity: maximum of $|v(t)|$
- Dominant frequency of velocity in three directions: $f_{v,dom,x}$, $f_{v,dom,y}$, $f_{v,dom,z}$
- Peak effective velocity in three directions: $v_{eff,x,max}$, $v_{eff,y,max}$, $v_{eff,z,max}$
- Peak effective velocity: $v_{eff,max}$ = maximum of ($v_{eff,x,max}$, $v_{eff,y,max}$, $v_{eff,z,max}$)

The peak vibration velocity of all buildings triggered by the Hellum earthquake is presented in Figure 5.3. A distinction is made between the horizontal (x,y) and the vertical (z) component of the vibration velocity.
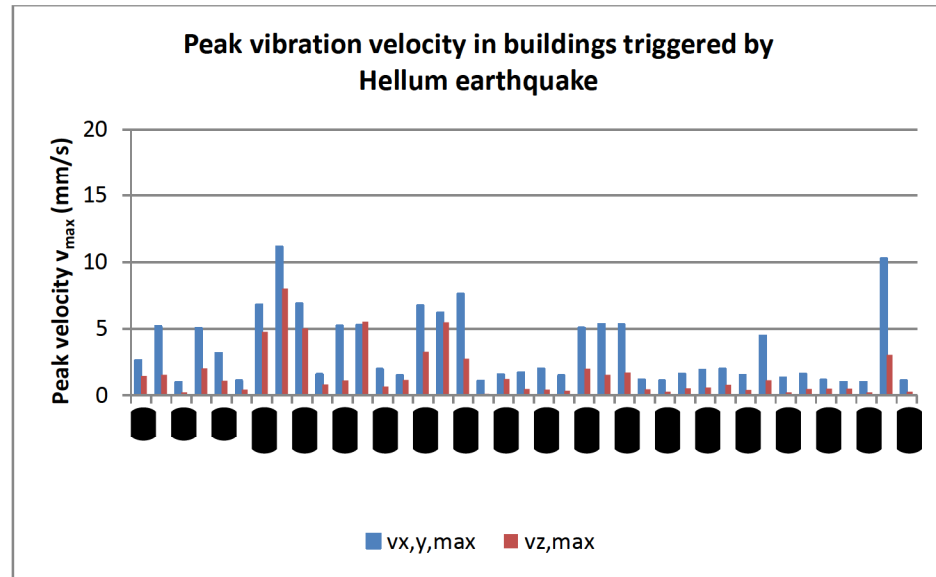
Figure 5.3: Peak velocity of all buildings triggered by the Hellum earthquake

The calculated vibration characteristics regarding the Cumulative Absolute Velocity are given in Annex F:
- Cumulative Absolute Velocity in three directions: CAV_x, CAV_y, CAV_z
- Total Cumulative Absolute Velocity: CAV_{total}
- Standardized Cumulative Absolute Velocity in three directions: $CAV_{STD,x}$, $CAV_{STD,y}$, $CAV_{STD,z}$
- Total Standardized Cumulative Absolute Velocity: $CAV_{STD,total}$

The calculated vibration characteristics regarding the Arias Intensity are given in Annex G:
- Arias Intensity in three directions: $I_{A,x}$, $A_{A,y}$, $A_{A,z}$
- Total Cumulative Arias Intensity: $I_{A,total}$

The horizontal and the vertical component of the vibration of each building are compared, to see which direction gives the highest vibrations. This is done for both the peak acceleration (Figure 5.4) and the peak velocity (Figure 5.5). For the Hellum earthquake the horizontal velocity is mostly dominant over the vertical velocity component. In case of the accelerations the vertical component this is not obvious and in many cases the vertical acceleration component is dominant over the horizontal one. The largest measured peak acceleration of 1.17 m/s^2 is in the vertical direction. Figure 5.6 shows the vertical to horizontal ratio for the accelerations versus the distance to the epicentre. The graph shows that higher ratios are observed near the epicentre and ratios are lower than one for larger distances from the epicentre.

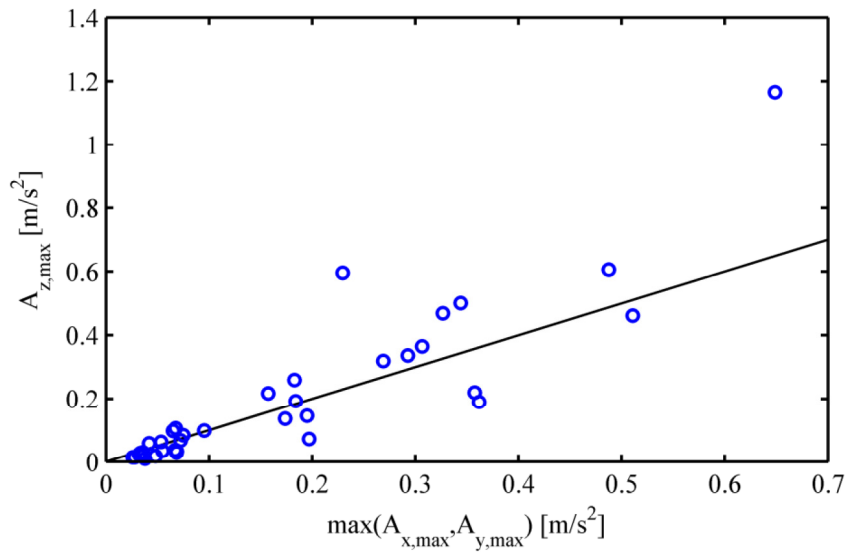Figure 5.4: *Horizontal versus vertical component of peak acceleration for all buildings triggered by the Hellum earthquake*
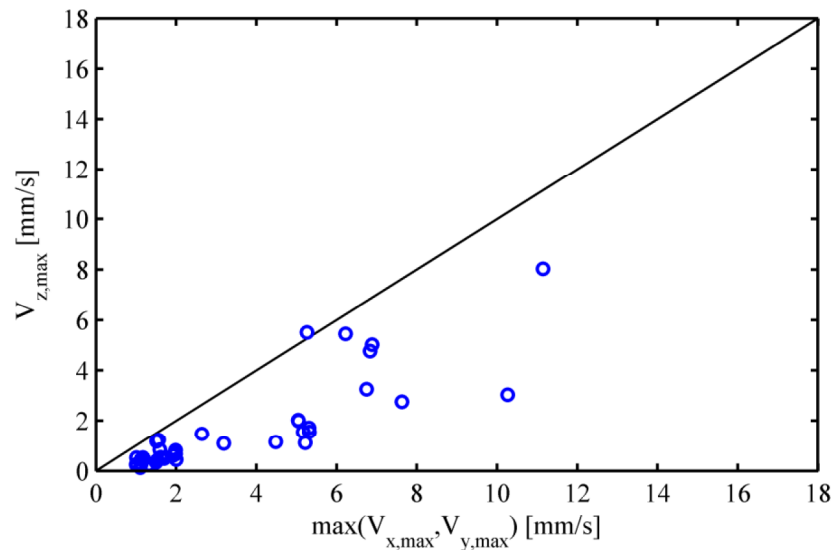

Figure 5.5: *Horizontal versus vertical component of peak velocity for all buildings triggered by the Hellum earthquake*
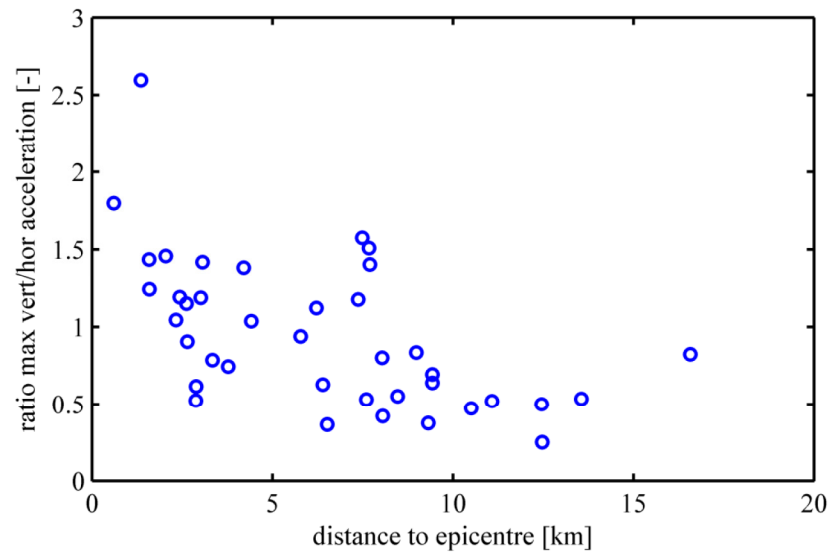
Figure 5.6:   Ratio of vertical to horizontal peak acceleration versus the distance to
              the epicenter for all buildings triggered by the Hellum earthquake

The peak acceleration and the peak velocity are compared to each other to look for
the relation between these two characteristics. The results of this comparison are
given in Figure 5.7. This Figure shows a rather linear relation between the peak
acceleration and the peak velocity for most of the buildings.

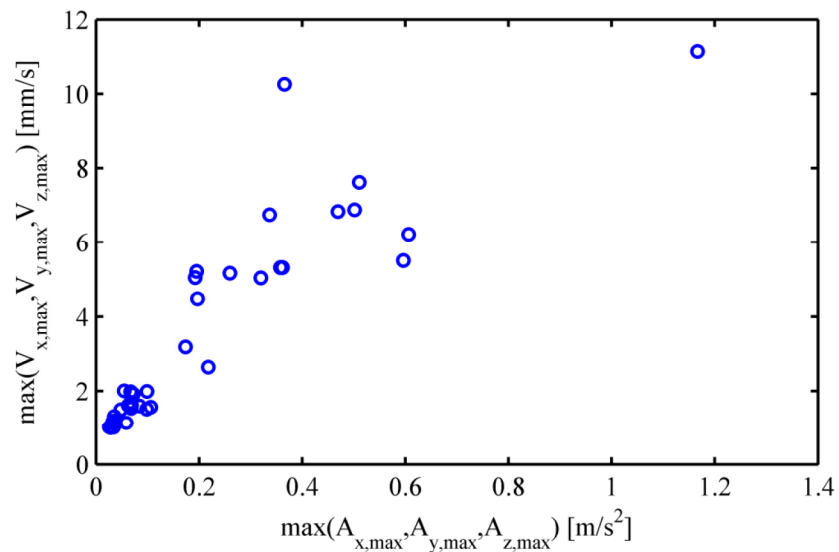Figure 5.7:   Peak acceleration versus the peak velocity for all buildings triggered
              by the Hellum earthquake

The distribution of the dominant frequency of the vibration accelerations is analysed
to make it possible to compare the dominant frequency of the ground-borne
vibrations with the ones of the foundations vibrations. The results of this analysis
are given in Figures 5.8 – 5.10.

The frequency spectra of the measured acceleration signals (see Annex B) show no significant frequency content above 25 Hz for the x- and y-channels for most sensors with some of the sensors which registered higher accelerations above 0.4 m/s^2 having frequency content up to 35-40 Hz. For the z-channel there is no significant content above 40 Hz for most sensors. But for the highest measured vertical acceleration of 1.17 m/s^2 the dominant frequency was 46.68 Hz and significant frequency content of up to 60 Hz is observed. As expected, the frequency spectra of the velocities (see Annex C) show a shift of the content to the lower frequencies with no significant content above 15 Hz for the x- and y-channels and above 25 Hz for the z-channel.

For the x- and y- channels, the dominant frequencies for acceleration are on average 8 Hz with a 95% upper bound of 12 Hz. For the z-channel the average dominant frequency is 19 Hz and the 95% upper bound is 45 Hz.

Figure 5.8: Distribution of dominant frequency of the vibration accelerations;
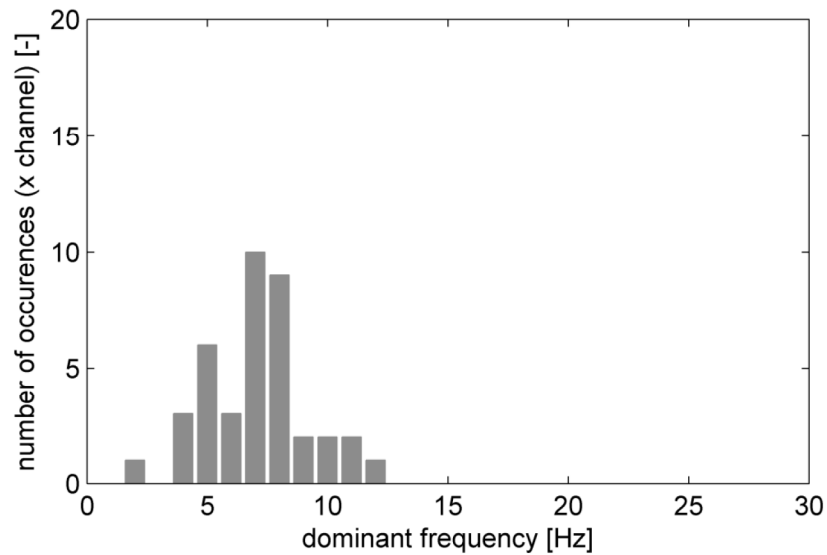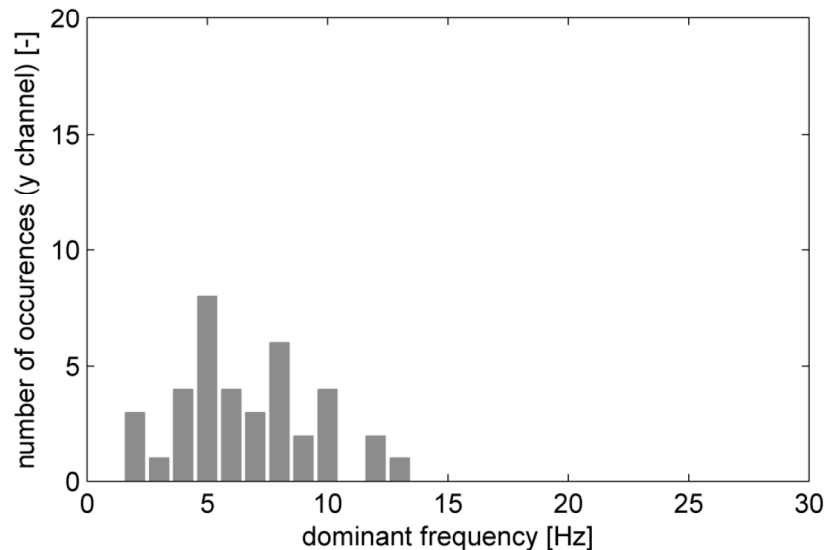*x-direction for all buildings triggered by the Hellum earthquake*

Figure 5.9: Distribution of dominant frequency of the vibration accelerations;
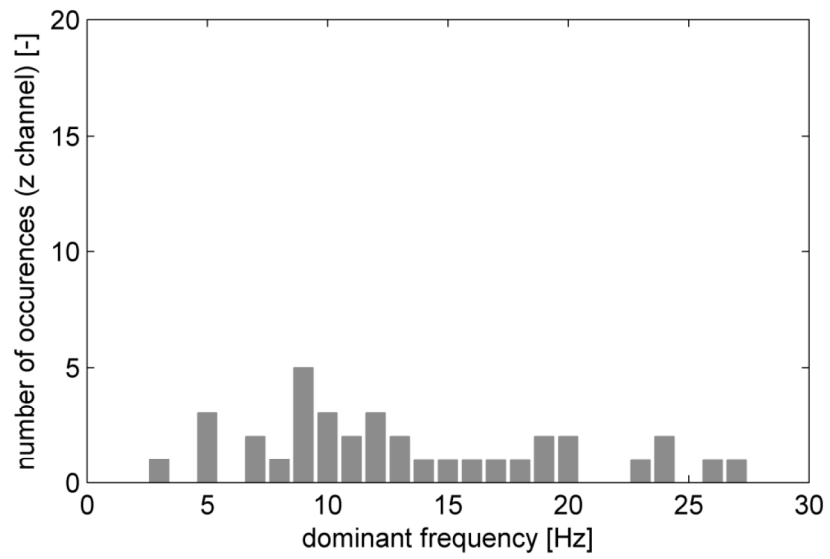*y-direction for all buildings triggered by the Hellum earthquake*

*Figure 5.10: Distribution of dominant frequency of the vibration accelerations;
z-direction for all buildings triggered by the Hellum earthquake*

6 Transfer functions

6.1 Introduction

For the Hellum event, Figure 6.1 below [06] shows all KNMI accelerograph stations in operation at the time of the Hellum event. Of these KNMI stations, the stations having an ID starting with the letter "G" are part of the new surface network of sensors installed in the field on small concrete plates. The other sensors are placed in "buildings" according to KNMI. To compare foundation vibrations with free surface vibrations the stations labelled with Gxx0 are used here, of which 33 were operational at the time of the Hellum event.

At the time of processing the KNMI sensor data for the Hellum event orientations of the horizontal axes are not yet determined for all KNMI stations. Most channels codes in the KNMI data are HG1 and HG2. According to KNMI, if the horizontal directions are "1" and "2", the orientation is not yet determined. For the processing it has not yet been possible to align the horizontal axes of the KNMI sensors with those of the TNO sensors for better comparison. Instead the vectorial maximum of the accelerations in the horizontal plane has been used in the comparisons.
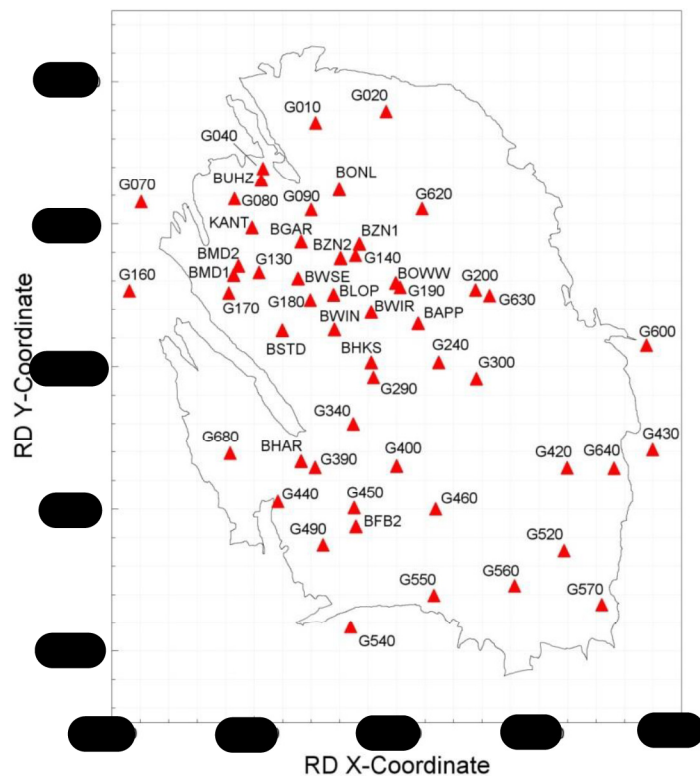
Figure 6.1: Location of the KNMI stations in the Groningen field ([06])

6.2 Results KNMI stations

Figure 6.2 shows the locations of the KNMI Gxx0 stations together with the locations of the TNO building sensors that have triggered during the Hellum event. The location of the epicentre is plotted as well. For the Hellum event the density of KNMI stations near the epicentre is rather low, while there are relatively more TNO sensors near the epicentre.

Table 6.1 provides the measured accelerations by the KNMI Gxx0 stations at the Hellum event: the vectorial maximum in horizontal direction and the maximum in vertical direction. These results show that two stations have a horizontal vectorial maximum of the accelerations of about 0.20 m/s^2 (station G300 and G400; encircled in Figure 6.2) and all others a value less than 0.05 m/s^2.

Table 6.1 also provide the distance of the KNMI stations to the closest TNO sensor. These distances show that only two KNMI stations are located at a distance less than 500 m to the nearest building with a TNO sensor. All other KNMI stations are located at a greater distance.

Figure 6.2: Locations of the KNMI Gxx0 stations and triggered TNO sensors during the Hellum event

Table 6.1: Measured accelerations by the KNMI Gxx0 stations

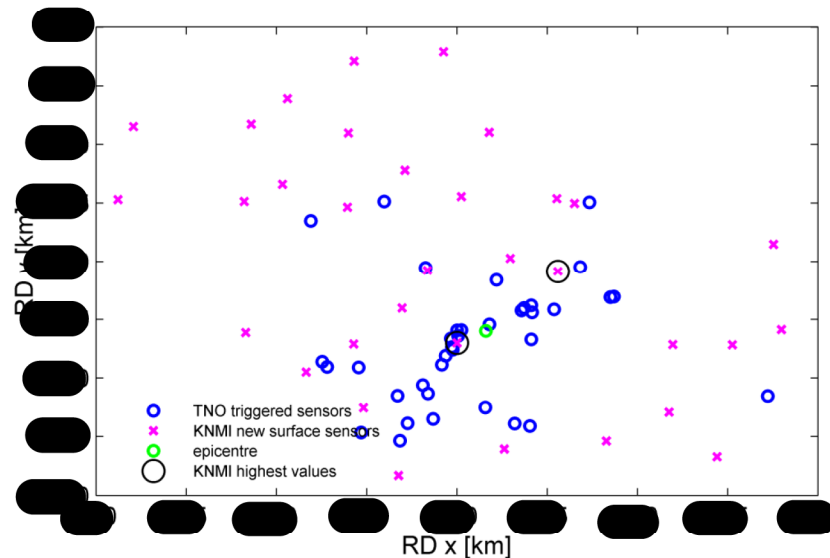| KNMI ID		RDX	RDY	$\|a(t)\|_{x,y-max}$	$a_{z,max}$	Distance to closest TNO sensor [km]
				(m/s^2)	(m/s^2)	
G	10	244310	607100	0.00	0.00	12
G	20	249260	607900	0.00	0.00	13
G	40	240610	603910	0.00	0.00	10
G	70	232070	601540	0.01	0.00	12
G	80	238600	601740	0.00	0.00	8
G	90	243990	600980	0.01	0.00	6
G	130	240340	596600	0.01	0.00	3
G	140	247120	597800	0.01	0.01	2
G	160	231220	595290	0.00	0.00	10
G	170	238210	595140	0.01	0.00	4
G	180	243930	594640	0.01	0.01	2
G	190	250240	595540	0.01	0.01	4
G	200	255540	595370	0.01	0.01	1
G	240	252960	590270	0.02	0.05	2
G	290	248360	589230	0.04	0.06	0
G	300	255590	589140	0.21	0.04	1
G	340	246960	585980	0.04	0.06	3
G	390	244280	582900	0.02	0.02	2
G	400	250000	582990	0.20	0.29	0
G	420	261960	582860	0.02	0.01	5
G	430	267980	584130	0.01	0.01	5
G	440	241650	580510	0.02	0.01	1
G	490	244820	577480	0.03	0.03	2
G	520	261750	577090	0.02	0.01	5
G	540	246770	571690	0.02	0.01	3
G	550	252620	573950	0.02	0.02	2
G	560	258280	574630	0.03	0.01	4
G	570	264410	573280	0.01	0.00	5
G	600	267540	591480	0.01	0.01	9
G	620	251790	601050	0.00	0.00	8
G	630	256510	594960	0.01	0.01	0
G	640	265260	582830	0.01	0.01	4
G	680	238290	583890	0.01	0.00	4

For a comparison between the measured accelerations by the KNMI stations and the TNO sensors the results of these measurements are presented together in Figure 6.3 and 6.4. Figure 6.3 presents the vectorial maximum in horizontal direction of both the KNMI stations and the TNO sensors, in relation to the distance to the epicentre of the Hellum earthquake. Figure 6.4 shows the same for the maximum in the vertical direction.
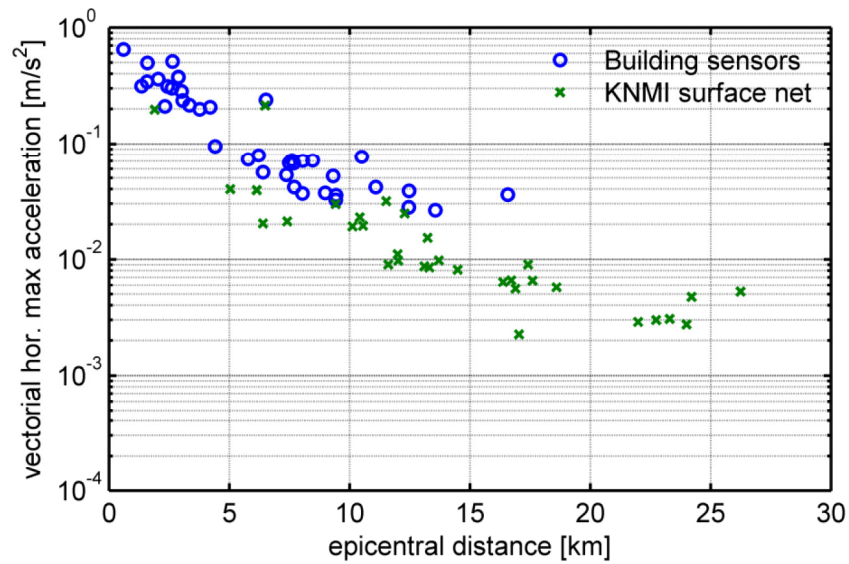
Figure 6.3: Vectorial maximum of horizontal acceleration versus epicentral distance.
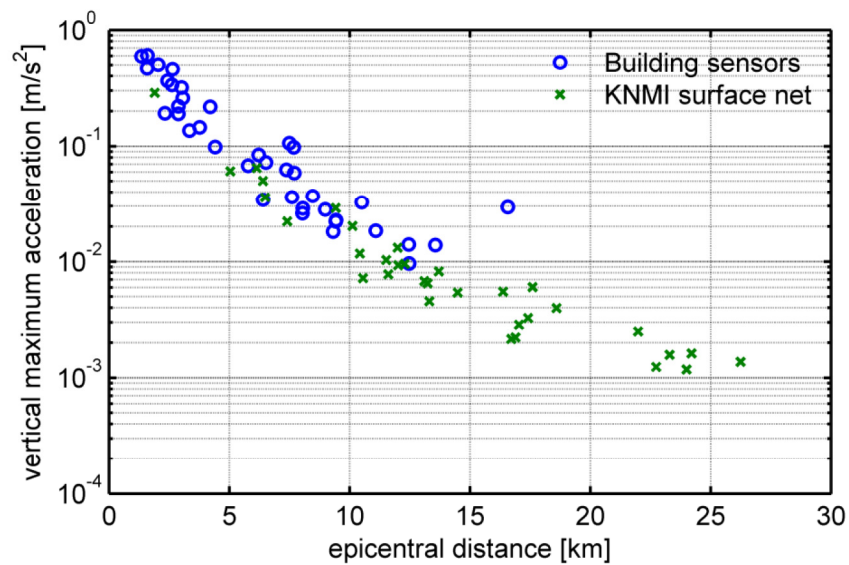
Figure 6.4: Maximum of vertical acceleration versus epicentral distance.

6.3 Transfer horizontal accelerations

This Paragraph gives an analysis of the transfer of the horizontal accelerations from the field (KNMI stations) to the foundation of the triggered buildings (TNO sensors). This is done for the following KNMI stations:

- Station G300 with the highest measured vectorial horizontal acceleration (0.21 m/s^2).
- Station G400 with the second highest measured vectorial horizontal acceleration (0.20 m/s^2) .
- Station G290 with a TNO sensor at a distance of 0.3 km.

For all other KNMI station the measured acceleration was too small or the distance to a TNO sensor was too big for a reliable analysis of the transfer of the accelerations.

6.3.1   *KNMI sensor G300*
There are 9 TNO sensors that are closer to KNMI sensor G300 than to another KNMI sensor. These 9 sensors are marked in Figure 6.5 with a pink colour.

Figure 6.5: Location of KNMI station G300 and the TNO sensors closest to it

KNMI sensor G300 has measured a vectorial maximum horizontal acceleration of 0.21 m/s^2. To compare this value to the measured building accelerations the following Figures are set up:

- Figure 6.6: This Figure shows a part of Figure 6.5, with the epicentre, the location of KNMI sensor G300 and the 9 TNO sensors nearest by. For each TNO sensor a value is given, presenting the ratio of the vectorial maximum of the horizontal acceleration of the TNO sensor divided by the one of KNMI station G300.
- Figure 6.7: This Figure is comparable to Figure 6.3 but with the 9 TNO sensors closest to KNMI station G300 marked with a pink colour.

The distance between KNMI station G300 and the nearest by TNO sensors is rather big (at least 1.3 km), so it is not possible to calculate a reliable transfer factor for the field acceleration to the individually measured foundation accelerations. In general, based on the trend of the acceleration levels with the distance to the epicentre (as shown in Figure 6.7), it seems that the nine TNO sensors show a lower horizontal acceleration than the acceleration measured by KNMI station G300.

Figure 6.6:   Location of KNMI station G300 and TNO sensors closest to it; the labels give the ratio of (vectorial) maximum of the horizontal acceleration of the TNO sensors versus KNMI station G300

Figure 6.7:   Maximum horizontal acceleration versus epicentral distance. Coloured in pink are KNMI sensor G300 and the nine closest TNO sensors

6.3.2   *KNMI senor G400*
There are 10 TNO sensors that are closer to KNMI sensor G400 than to another KNMI sensor. These 10 sensors are marked in Figure 6.8 with a pink colour.
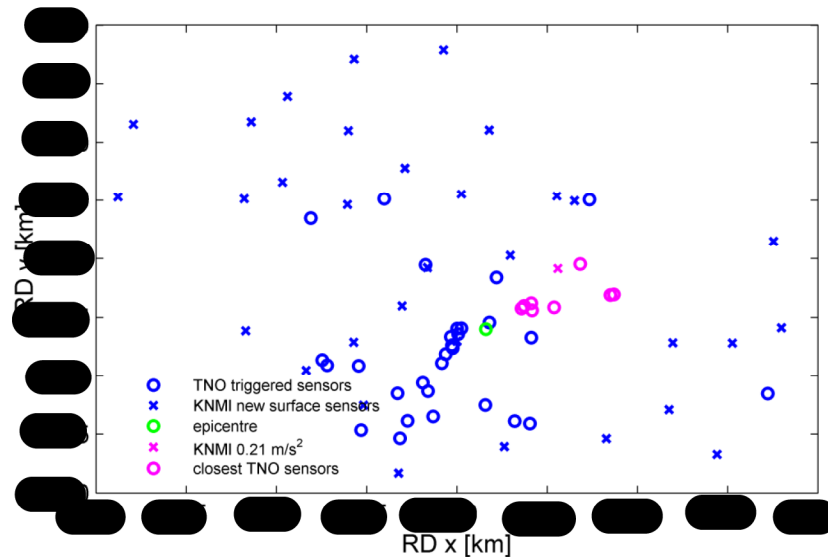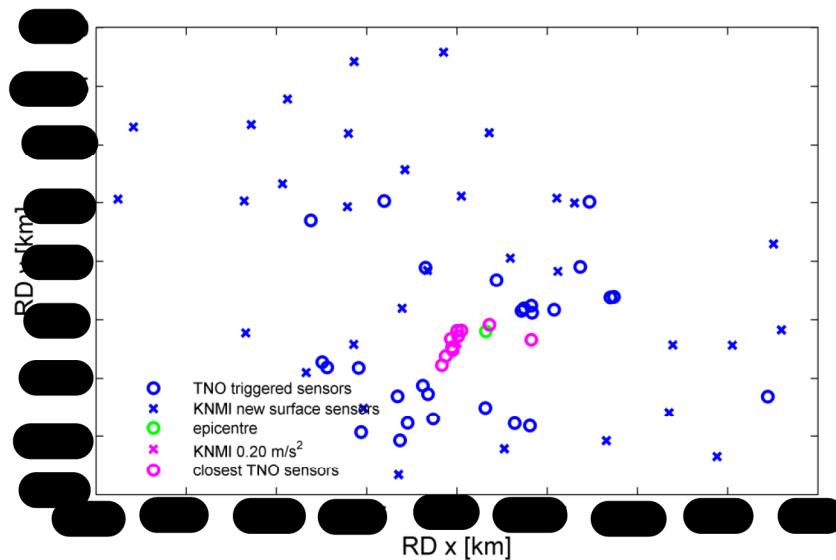
Figure 6.8: Location of KNMI station G400 and the TNO sensors closest to it

KNMI sensor G400 has measured a vectorial maximum horizontal acceleration of 0.20 m/s^2. To compare this value to the measured building accelerations the following Figures are set up:

- Figure 6.9: This Figure shows a part of Figure 6.8, with the epicentre, the location of KNMI sensor G400 and the 10 TNO sensors nearest by. For each TNO sensor a value is given, presenting the ratio of the vectorial maximum of the horizontal acceleration of the TNO sensor divided by the one of KNMI station G400.
- Figure 6.10: This Figure is comparable to Figure 6.3 but with the 10 TNO sensors closest to KNMI station G400 marked with a pink colour.

The distance between KNMI station G400 and the nearest by TNO sensors is rather big (at least 0.4 km), so it is not possible to calculate a reliable transfer factor for the field acceleration to the individually measured foundation acceleration. In general, based on the trend of the acceleration levels with the distance to the epicentre (as shown in Figure 6.10), it seems that the ten TNO sensors show a higher horizontal acceleration than the acceleration measured by KNMI station G400.
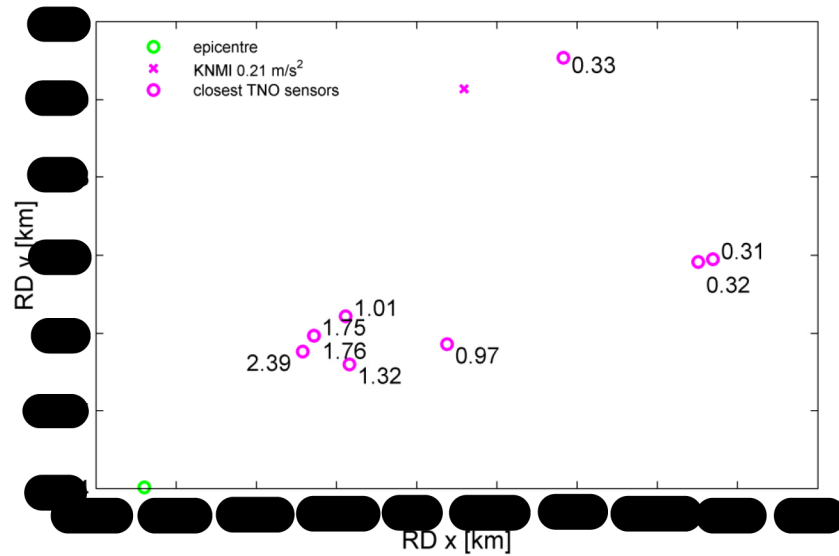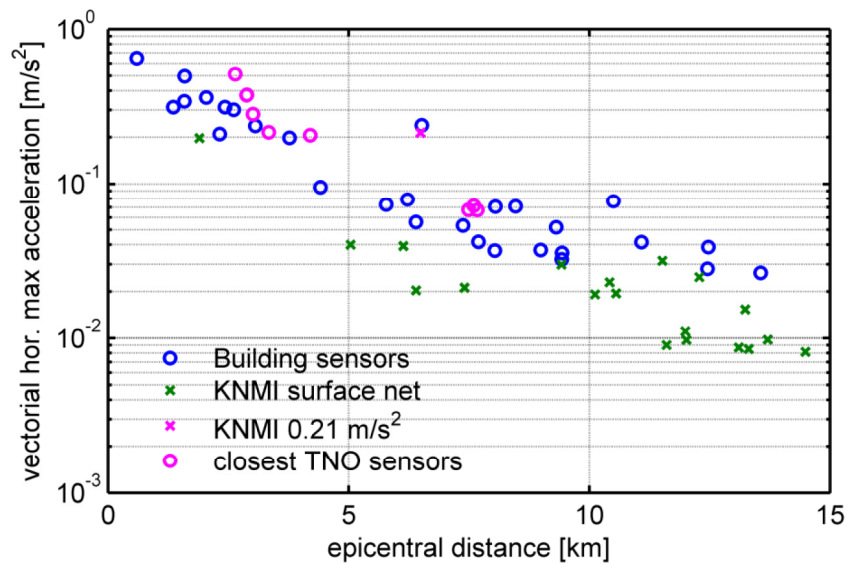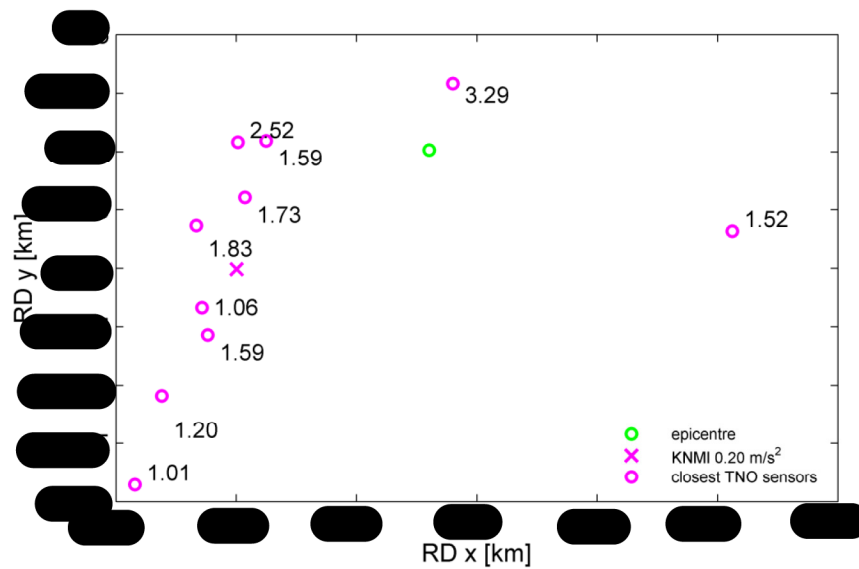
Figure 6.9:   *Location of KNMI station G400 and TNO sensors closest to it; the labels give the ratio of (vectorial) maximum of the horizontal acceleration of the TNO sensors versus KNMI station G400*

Figure 6.10: *Maximum horizontal acceleration versus epicentral distance. Coloured in pink are KNMI sensor G400 and the ten closest TNO sensors*

6.3.3   KNMI sensor G290

KNMI sensor G290 has measured a vectorial maximum horizontal acceleration of 0.04 m/s^2. The nearest by TNO sensor, at a distance of 0.3 km, has measured a vectorial maximum horizontal acceleration of 0.06 m/s^2. This is a ratio of the TNO sensor versus the KNMI station of 1.5, although the mutually distance between these two is rather small in comparison to the distance to the epicentre (about 6.2 km).

6.3.4   *Conclusions*
From the analysis of the transfer of the horizontal accelerations from the field (KNMI stations) to the foundation of the triggered buildings (TNO sensors) the following conclusions can be drawn:
- The distance between the KNMI stations and the nearest by TNO sensors is rather big, so it is not possible to calculate reliable transfer factors for individual buildings.
- The two KNMI stations with the highest measured accelerations show a different behaviour in comparison to the accelerations measured by the TNO sensors. For one KNMI station it seems the TNO sensors show a higher horizontal acceleration than the acceleration measured by KNMI station and for the other one a lower horizontal acceleration (based on the trend of the acceleration levels with the distance to the epicentre).

6.4   Transfer vertical accelerations

This Paragraph gives an analysis of the transfer of the vertical accelerations from the field (KNMI stations) to the foundation of the triggered buildings (TNO sensors). This is done in the same way as for the horizontal accelerations, for the following KNMI stations:
- Station G300 with the highest measured vectorial horizontal acceleration (0.21 m/s^2), but a rather low vertical acceleration (0.04 m/s^2).
- Station G400 with the second highest measured vectorial horizontal acceleration (0.20 m/s^2) and the highest measured vertical acceleration (0.29 m/s^2) .
- Station G290 with a TNO sensor at a distance of 0.3 km.

For all other KNMI station the measured acceleration was too small or the distance to a TNO sensor was too big for a reliable analysis of the transfer of the accelerations.

Figures 6.11 and 6.12 show the same plots for the vertical acceleration as the plots provided in Figure 6.7 and 6.10 for the horizontal accelerations.
The distance between the KNMI station G300 and G400 and the nearest by TNO sensors is rather big, so it is not possible to calculate a reliable transfer factor for the field acceleration to the individually measured foundation acceleration (see paragraph 6.3). In general, based on the trend of the acceleration levels with the distance to the epicentre (as shown in Figure 6.11 and 6.12), it seems that the TNO sensors show a higher vertical acceleration than the acceleration measured by the KNMI stations G300 and G400.

KNMI sensor G290 has measured a maximum vertical acceleration of 0.06 m/s^2. The nearest by TNO sensor, at a distance of 0.3 km, has measured a maximum vertical acceleration of 0.03 m/s^2. This is a ratio of the TNO sensor versus the KNMI station of 0.5, although the mutually distance between these two is rather small in comparison to the distance to the epicentre (about 6.2 km).
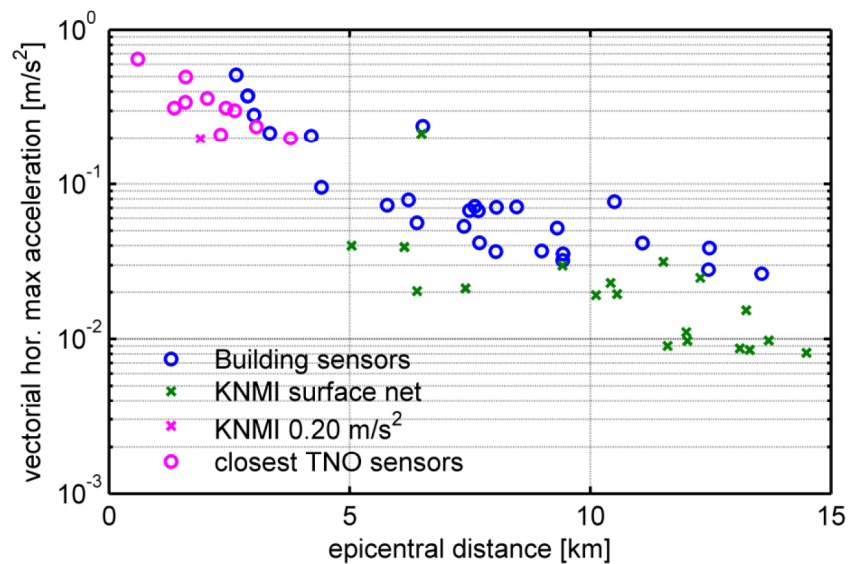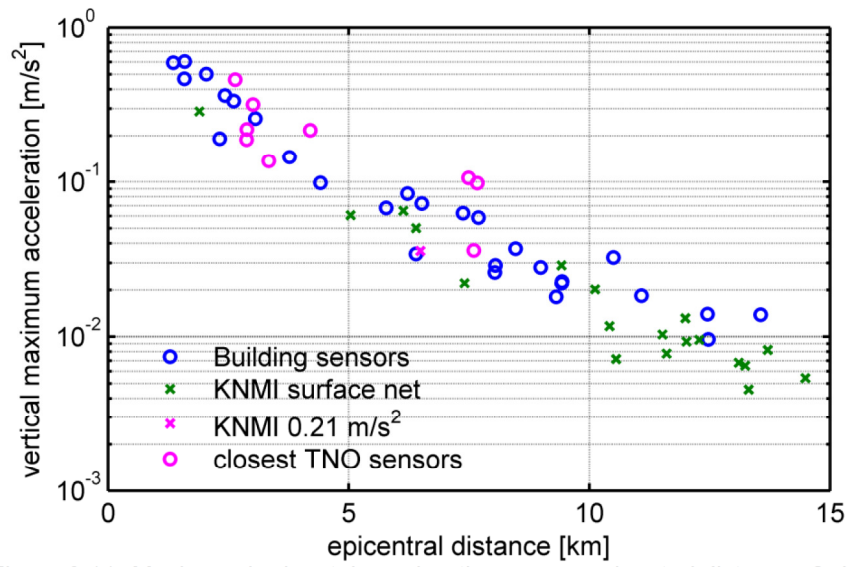
Figure 6.11: Maximum horizontal acceleration versus epicentral distance. Coloured in pink are KNMI sensor G300 and the nine closest TNO sensors
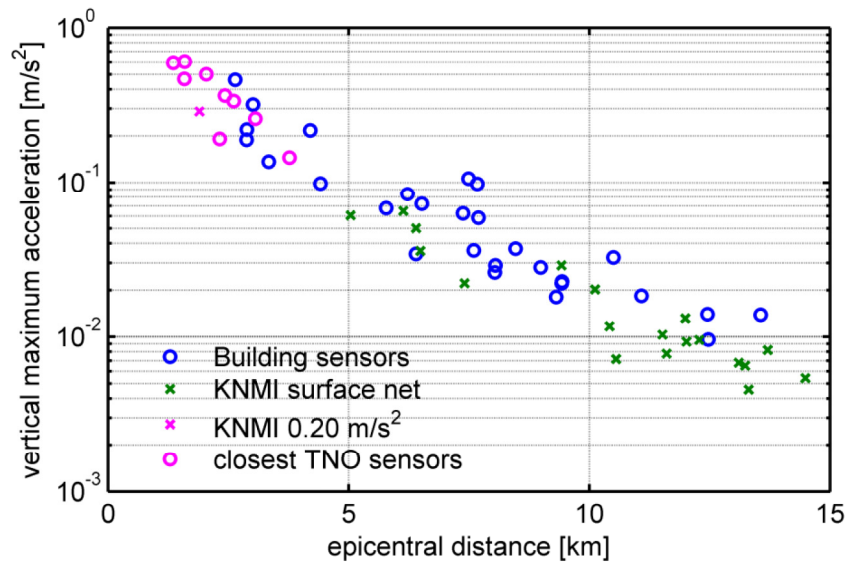

Figure 6.12: Maximum vertical acceleration versus epicentral distance. Coloured in pink are KNMI sensor G400 and the ten closest TNO sensors

7 Framework analysis damage of buildings

7.1 General

During the installation of the sensors, an initial damage survey of the buildings has been executed (see TNO-report "Monitoring Network Building Vibrations"; Chapter 11 (ref [01])). The main aim of this damage survey was to classify the initial damage in the buildings according to the EMS-98 "European Seismological Scale" (see Figure 7.1 and Table 7.1). This damage scale was used to comply with the setup of the fragility curves for the building stock in the Groningen region (see ARUP report "Seismic Risk Study Earthquake Scenario-Based Risk Assessment" d.d. 29 November 2013) and since this classification has been used in many other damage studies across Europe.

The initial building damage survey was limited to a survey of the cracks in the external parts of the building facades, because this information is sufficient for the categorisation of the building damage according to the EMS-scale.
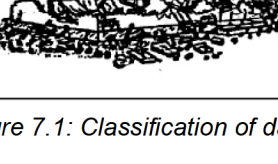
Classification of damage to masonry buildings	
	Grade 1: Negligible to slight damage (no structural damage, slight non-structural damage) Hair-line cracks in very few walls. Fall of small pieces of plaster only. Fall of loose stones from upper parts of buildings in very few cases.
	Grade 2: Moderate damage (slight structural damage, moderate non-structural damage) Cracks in many walls. Fall of fairly large pieces of plaster. Partial collapse of chimneys.
	Grade 3: Substantial to heavy damage (moderate structural damage, heavy non-structural damage) Large and extensive cracks in most walls. Roof tiles detach. Chimneys fracture at the roof line; failure of individual non-structural elements (partitions, gable walls).
	Grade 4: Very heavy damage (heavy structural damage, very heavy non-structural damage) Serious failure of walls; partial structural failure of roofs and floors.
	Grade 5: Destruction (very heavy structural damage) Total or near total collapse.

Figure 7.1: Classification of damage for masonry buildings (EMS-98)

Table 7.1: Defined damages state of buildings

Damage state	Description
DS 0	No damage
DS 1	Negligible damage ("non-structural")
DS 2	Moderate damage ("slight structural")
DS 3	Substantial to heavy damage ("structural")
DS 4	Very heavy damage
DS 5	Destruction

7.2 Repetitive building survey

After an earthquake, all buildings triggered by that earthquake have been surveyed again, in a similar way as the initial damage survey. The registration form used for this repetitive damage survey is given in Annex H.

During this repetitive damage survey cracks that were already present have been examined:
- to see if the length and/or the width has been increased
- to see if they are repaired in the meantime
- to see if repaired cracks have cracked again.

Also new cracks are reported, in the same way as during the initial damage survey.

Based on the results of the repetitive damage survey the damage state of the buildings after the earthquake has been determined.

7.3 Damage curves

Based on a comparison of the initial building damage state and the damage state after the earthquake, the effect of the earthquake on the individual buildings can be determined. Subsequently this effect can be related to the measured vibration level of the foundation during the earthquake.

The relation between vibration level and occurred damage can be characterized in different ways. In line with the SBR directive for vibration damage (ref [02]) the vibration level will be characterized by the peak velocity of the buildings. Therefore, damage curves have been setup based on the relation between the peak velocity of the building foundations and the damage state after the earthquake.

If sufficient data is available, also other damage curves will be made, based on other characterizations of the vibrations, such as:
- Peak ground acceleration (KNMI; in line with the fragility curves)
- Peak acceleration
- Vectorial maximum of the acceleration
- Vectorial maximum of the velocity.

In the period between the previous damage survey and the current damage survey, other vibrations could have occurred in the buildings. This could be vibrations due to an other earthquake, which took place in the intermediate period. This could also be triggers other than an earthquake. If these have occurred, the building owners were asked for the reason for this trigger.

Other vibrations will affect the results. Either the recorded vibration level is too low for the damage state, or the damage state is not the result of the considered earthquake. The maximum measured building vibration levels in the period between the two damage surveys has been used for the damage curves.

8   Repetitive damage survey buildings

The repetitive damage surveys have taken place from October 19th 2015 till October 30th 2015. For a total of 40 houses the repetitive damage survey was scheduled, however:

- for 1 triggered house the survey was cancelled, because repair activities took place, for which the masonry joints were removed (ID■);
- for 1 triggered house the survey was cancelled, because the owner could not be contacted (ID■);
- for 1 triggered house, repair activities took place between the earthquake and the survey (ID■). Therefore observations regarding damage increase could not be made. However, new pictures were taken for future damage analysis.

The results of these repetitive damage surveys are given in Annex I. For each building this Annex provides the following information:

- The amount of cracks registered at the previous damage survey, for each of the three categories of crack width separately (category A < 1 mm; category B between 1 and 10 mm; category C > 10 mm).
- The amount of cracks with an increase in length and/or width, divided in cracks that remained in the same category of crack width and cracks which moved to a higher category.
- The amount of new cracks registered for each of the three categories of crack width A, B and C.
- Remarks regarding the repetitive damage survey.

Note:
The purpose of the initial survey was to detect and record major cracks in the buildings, in order to determine the damage state (DS) of the buildings. At that time it was not intended to execute a total survey, including also the smallest cracks.
During the first repetitive surveys question raised, mainly about small cracks, whether these crack were already present or were caused by the earthquake. For this reason it was decided to record also minor cracks. As a consequence of this decision the first repetitive surveys show much more cracks than the initial survey.

The repetitive damage survey of 37 houses resulted in the following additional information:

- In the previous damage survey, a total amount of 384 cracks was reported for the 37 buildings. The repetitive damage survey has shown that 4 of these cracks have increased in width and/or in length.
- Most of the new reported cracks were relatively small and short and belong to crack width category A.
- A large part of the new reported cracks is located at the lintels and the sills of windows and doors.
- From overview photos of the facades, taken at the initial damage survey, it could be verified that several new reported cracks were already present at the initial damage surveys, but were not reported at that time.
- Based on the previous remark it is expected that more new reported cracks (at the first repetitive damage survey) were already present at the initial damage survey.

Based on the results of the repetitive damage survey, the damage state of the buildings after the Hellum earthquake has been categorized again. The results of the categorization of the last damage state and the damage state after the Hellum earthquake are presented in Table 8.1.

Table 8.1: Categorization of the previous damage state and the damage state at the repetitive damage survey

ID	Peak vibration velocity $v_{x,y,max}$ (mm/s)	Damage state (DS)	
		At previous damage survey	At repetitive damage survey
■	2.6	2	2'
■	5.2	1	0
■	1.0	1	1'
■	5.0	1	1'
■	3.2	1	1'
■	1.1	1	1
■	11.1	2	2
■	6.9	1	1'
■	5.2	2	2'
■	5.3	2	2'
■	2.0	1	1'
■	1.5	2	2'
■	6.7	1	1
■	6.2	1	1'
■	5.0*	2	2'
■	7.6	1	1
■	1.1	1	1
■	1.6	1	1
■	1.7	1	1'
■	1.5	1	1
■	5.0*	1	1
■	5.1	1	1
■	5.3	1	1'
■	5.3	1	1'
■	1.2	1	1
■	1.1	1	1'
■	1.6	1	1
■	1.9	2	2'
■	1.0	0	1
■	2.0	2	2'
■	1.5	1	1
■	4.5	1	1
■	1.3	1	1
■	1.6	1	1'
■	1.2	1	1'
■	1.0	2	2'

ID	Peak vibration velocity $v_{x,y,max}$ (mm/s)	Damage state (DS)	
		At previous damage survey	At repetitive damage survey
⬛	1.1	1	1'

* = estimated value, based on vibration level nearby houses

9 Analysis repetitive damage survey

9.1 Normative vibration velocity

For the period between the last damage survey and the repetitive damage survey, the buildings triggered by the Hellum earthquake have been scanned for other triggers. In addition, building owners were asked for a possible explanation. For some buildings, the vibration level caused by another source was higher than that caused by the Hellum earthquake. In case of a local vibration, such as mounting the sensor's cover lit, these registered vibrations are excluded for damage analysis. In case of a vibration for which it is likely that it resulted in a vibration of the whole building, it is taken into account for damage analysis.

An overview of buildings for which vibration velocities have been registered which have exceeded the level of those registered during the earthquakes is given in Table 9.1.

Table 9.1: Buildings for which a vibration velocity is registered that has exceeded the registered vibration velocity during the earthquake

ID	Maximum registered vibration velocity		
	Earthquake Hellum	Other triggers (maximum value of both vertical and horizontal component)	Taken into account
	$v_{x,y,max}$ (mm/s)	$v_{x,y,z,max}$ (mm/s)	$v_{x,y,max}$ (mm/s)
⬛	2.6	1 trigger 24 mm/s: bump against sensor 1 trigger 42 mm/s: bump against sensor This level is not taken into account	2.6
⬛	5.2	4 triggers 17 mm/s < x < 77 mm/s: bump against sensor This level is not taken into account	5.2
⬛	1.0	1 trigger 1.9 mm/s: bump against sensor This level is not taken into account	1.0
⬛	1.1	8 triggers 1.1mm/s < x < 1.9 mm/s: Causes unknown / building activities	1.9
⬛	5.2	1 trigger 45 mm/s: bump against sensor This level is not taken into account	5.2
⬛	1.5	5 triggers 1.5 mm/s < x < 2.6 mm/s causes: repair work (joints) and tree falling (building owner felt a shock when tree hit the ground) It is expected that a tree hitting the ground, will likely cause a vibration of the whole building. Therefore this level is taken into account.	2.6
⬛	5.0*	5 triggers 1.5 mm/s < x < 2.6 mm/s causes: repair works on roof and gutter This level is not taken into account.	5.0

ID	Maximum registered vibration velocity		
	Earthquake Hellum	Other triggers (maximum value of both vertical and horizontal component)	Taken into account
	$V_{x,y,max}$ (mm/s)	$V_{x,y,z,max}$ (mm/s)	$V_{x,y,max}$ (mm/s)
⬛	7.6	1 trigger 8.9 mm/s, 1 trigger 19 mm/s cause: cavity wall insulation. This level is not taken into account	7.6
⬛	1.2	1 trigger 2.5 mm/s: nearby buidling activities. his vibration level is taken into account	2.5
⬛	1.5	1 trigger 4.2 mm/s; building activities (own house). This level is not taken into account	1.5
⬛	1.3	4 triggers 1.3 mm/s < x < 8.1 mm/s: building activities (own house). This level is not taken into account	1.3

9.2 Damage curves

The damage curves of the Hellum earthquake are given for the three damage state categories (Figure 9.1 – 9.3). The horizontal axis in the figures shows the maximum registered vibration velocity in horizontal direction in the period between the previous and the repetitive damage survey (see Table 8.1 and 9.1). The vertical axis shows the damage state categories according to the following scheme:

Buildings categorized in DS 0 at previous survey
- DS 0→DS 0 = remained in DS 0
- DS 0→DS 1 = damage stated increased to DS 1
- DS 0→DS 2 = damage stated increased to DS 2

Buildings categorized in DS 1 at previous survey
- DS 1→DS 0 = repaired to DS 0 and remained in DS 0
- DS 1→DS 1 = remained in DS 1
- DS 1→DS 1' = remained in DS 1, but increase in amount and/or length and/or width of cracks
- DS 1→DS 2 = damage state increased to DS 2

Buildings categorized in DS 2
- DS 2→DS 1 = repaired to DS 1 and remained in DS 1
- DS 2→DS 2 = remained in DS 2
- DS 2→DS 2' = remained in DS 2, but increase in amount and/or length and/or width of cracks
- DS 2→DS 3 = damage state increased to DS 3

Buildings categorized in DS 3
- DS 3→DS 3 = remained in DS 3
- DS 3→DS 3' = remained in DS 3, but increase in amount and/or length and/or width of cracks
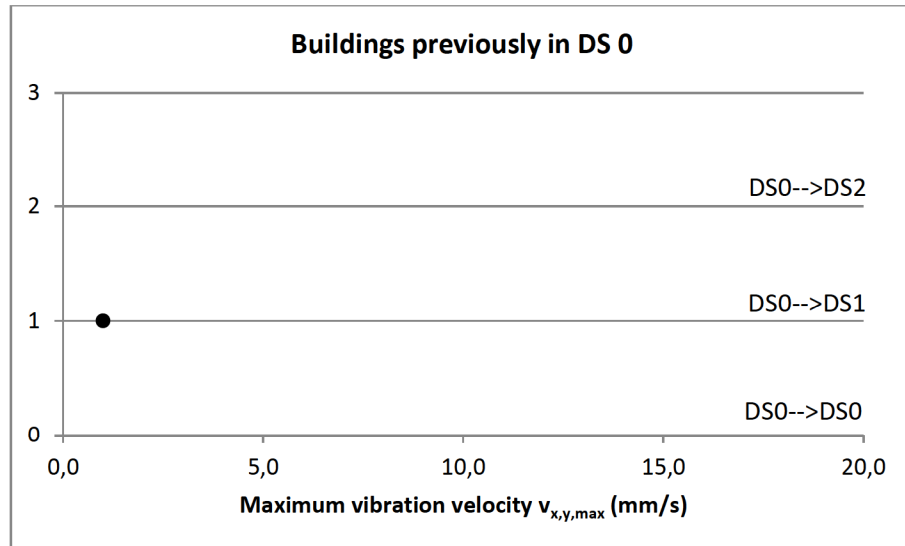
Figure 9.1: Damage state for buildings categorised in DS 0 at last survey
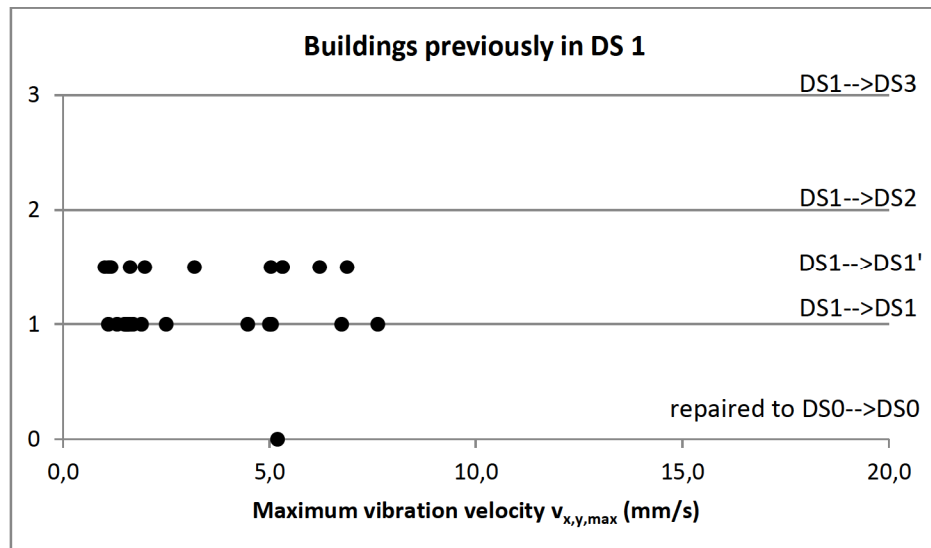
Figure 9.2: Damage state for buildings categorised in DS 1 at last survey
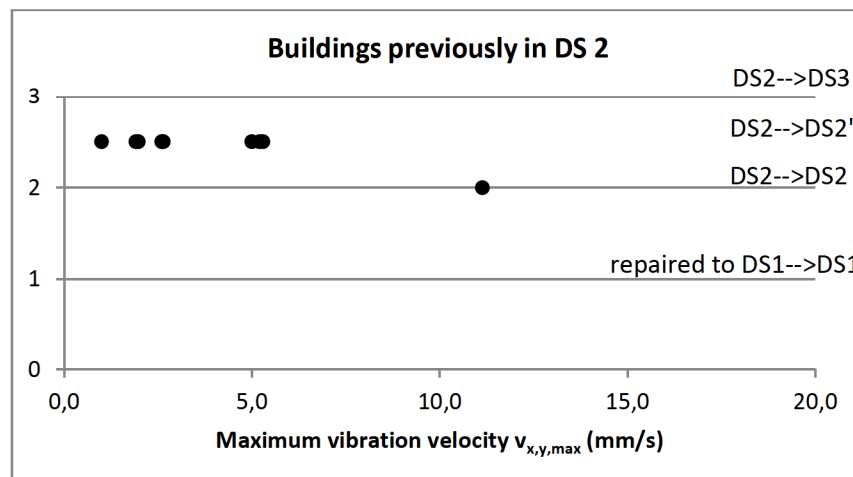
Figure 9.3: Damage state for buildings categorised in DS 2 at last survey

9.3   Conclusions damage curves

From the damage curves presented in the former Paragraph (Figures 9.1 – 9.3) the following conclusions can be drawn:

- For the building that was categorised in damage state DS 0 (ID███), having no reported cracks, one new cracks was reported. Therefore this building was categorized in the new category DS 1. However, the newly reported crack was already present at the time of the initial damages survey. Because of this, this building was initially already in DS 1.
- For all buildings categorized in damage state DS 1 and DS 2 the earthquakes didn't result in an increase of the damage state. This means that the missed cracks at the initial or previous damage survey had no influence on the previous categorization of the damage state of the buildings.
- For one building in DS1 (ID███) substantial repair activities have taken place in the period between the repetitive damage survey and the previous survey. As a consequence, the damage state has "improved" to DS 0.
- For more buildings repair activities have taken place in between the two surveys, but these were too limited in order to decrease the building's damage state. Most of the repaired cracks did not show new cracking after the earthquake (Tables 9.2).

Table 9.2: Repair activities

ID	$v_{x,y,max}$ (mm/s)	Behaviour of repair works
██	5.2	The existing crack was repaired; no new crack
██	1.9	17 existing cracks were repaired; no new crack
██	5.3	4 existing cracks were repaired; one showed a hair crack, the others no new crack
██	2.6	10 existing cracks were repaired; no new crack
██	7.6	1 existing crack was repaired; no new crack

10   Conclusions

TNO has analysed the effects of the Hellum earthquake of the 30th September 2015 on the buildings of the monitoring network. The analysis has resulted in the following conclusions.

Building vibrations

1.   In 40 buildings of the monitoring network the maximum building vibration velocity of the foundation has exceeded the pre-set trigger of 1 mm/s.

2.   The maximum measured foundation vibration acceleration (a_{max}) is 1.17 m/s^2 in the vertical direction and 0.65 m/s^2 in the horizontal direction.

3.   The maximum measured foundation vibration velocity (v_{max}) is 11.14 mm/s in the horizontal direction.

4.   The horizontal component of the vibrations is dominant over the vertical component, for the velocity. For acceleration in many instances the vertical component is dominant over the horizontal, in particular for buildings close to the epicentre.

5.   For the x- and y-direction of the buildings, the dominant frequency is on average 8 Hz. The dominant frequency for the z-direction is on average 19 Hz.

6.   The analysis of the transfer of the accelerations from the field (KNMI stations) to the foundation of the triggered buildings (TNO sensors) has shown that the distance between the KNMI stations and the nearest by TNO sensors is rather big, so it is not possible to calculate reliable transfer factors for individual buildings.

Repetitive damage survey

7.   The analysis of the damage survey was executed for 37 buildings.

8.   From these 37 buildings, a total amount of 384 cracks was reported. At the repetitive damage survey only 4 of these cracks were increased in length or width.

9.   The majority of the newly reported cracks were relatively small and short cracks of category A.

10. Several new reported cracks were already present at the initial damage surveys, but were not reported at that time.

11. For all buildings that were initially (or at previous survey) categorized in damage state DS 1 and DS 2, the earthquakes didn't result in an increase of damage state. This means that the missed cracks at the initial damage survey had no influence on the initial categorization of the damage state of these buildings.

12. At one buildings repair activities have taken place in the period between the repetitive damage survey and the previous damage survey. For this building the damage state has decreased as a consequence of these repair activities.

11   References

[01] TNO-report 2015 R10501 "Monitoring Network Building Vibrations"

[02] SBR guide line A: "Trillingen: meet- en beoordelingsrichtlijnen. Schade aan gebouwen, 2002"

[03] SBR guide line B: "Meet- en beoordelingsrichtlijn. Hinder voor personen in gebouwen, 2002"

[04] TNO-report 2015 R10604 "Monitoring Network Building Vibrations – Analysis Earthquake 30-09-2014 Garmerwolde"

[05] TNO-report 2015 R11382 "Monitoring Network Building Vibrations – Analysis Earthquakes 05-11-2014 (Zandeweer), 30-12-2014 (Woudbloem) and 06-01-2015 (Wirdum)"

[06] Ground-Motion Records from additional earthquakes recorded by the KNMI Accelerograph Network in the Groningen Field Michail Ntinalexis, Julian J Bommer & Bernard Dost, Version 0, 19 October 2015

12   Signature

Name and address sponsor:

Nederlandse Aardolie Maatschappij
PO Box 28000
9400 HH Assen

Signature:

Signature Research Manager Structural Reliability a.i.:

A   Background information

Table A.1: Building types

No.	Building type	Foundation	Type of floor
1	Terraced building - corner	(Piles)[1]	(Concrete)[1]
2	Terraced building – no corner	(Piles)[1]	(Concrete)[1]
3	Semi-detached	(Piles)[1]	(Concrete)[1]
4	Detached <1940	No piles	Combination wood/concrete
5		No piles	Wood
6		No piles	Concrete
7	Detached 1941-1975	No piles	--
8	Detached >1975	Piles	Concrete
9		No piles	Concrete
0	Other (not a house; most of them public buildings)		

)[1] Not all buildings fulfil this pre-set properties (see TNO-report 2015 R10501 "Monitoring Network Building Vibrations" [01])

B Vibration signals – acceleration

This Annex gives an example of the measured vibration acceleration signals. For four buildings, with different levels of acceleration, the following graphs are given:

- Measured acceleration (a_x, a_y, a_z)
- Distribution of the frequency ($f_{dom,a,x}$, $f_{dom,a,y}$, $f_{dom,a,z}$)
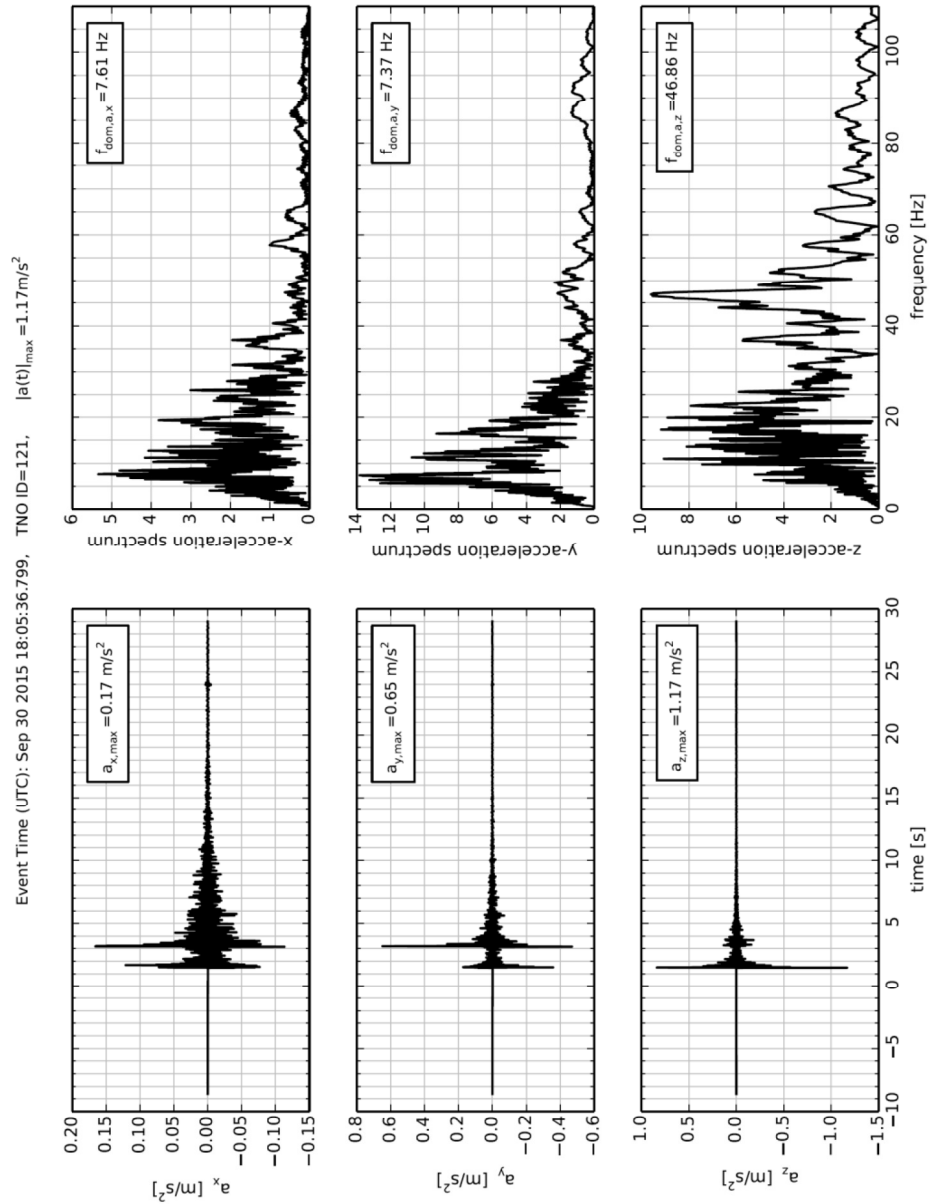
Event Time (UTC): Sep 30 2015 18:05:36.799, TNO ID=309, $|a(t)|_{max} = 0.52 m/s^2$
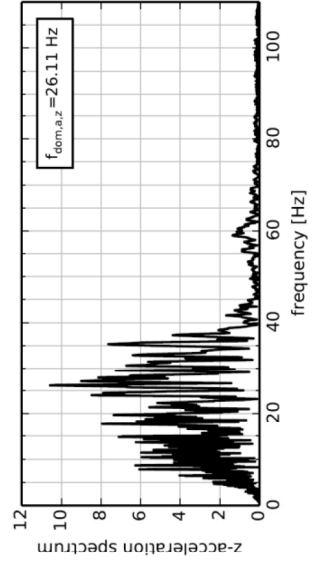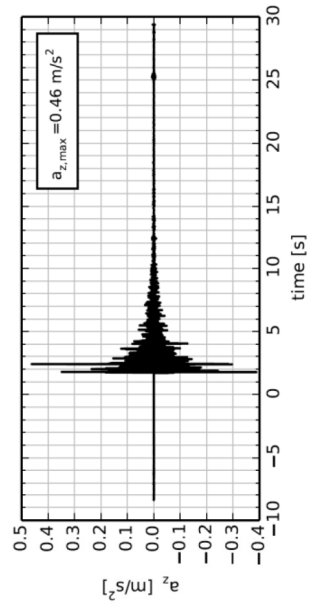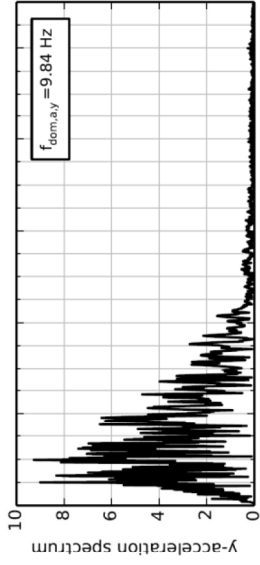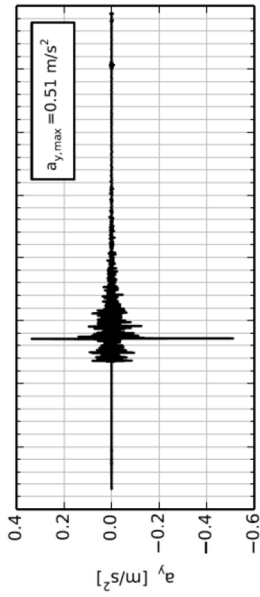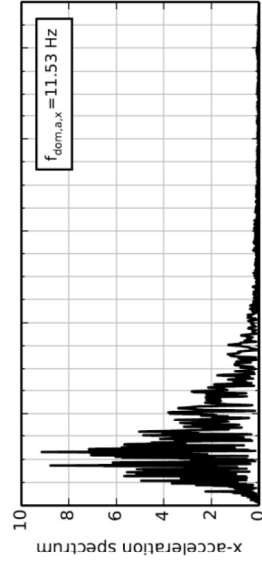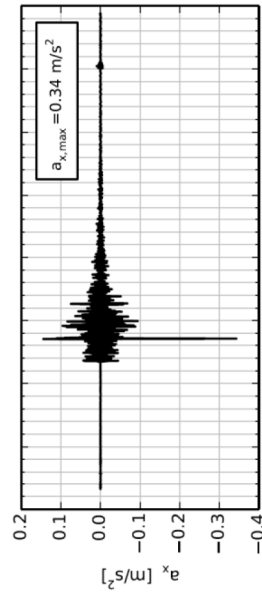
Event Time (UTC): Sep 30 2015 18:05:36.799, TNO ID=36, $|a(t)|_{max}$ =0.26m/s²
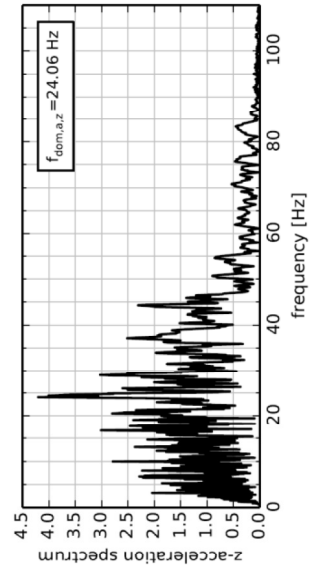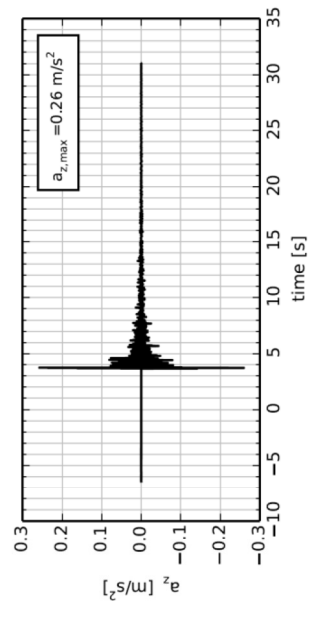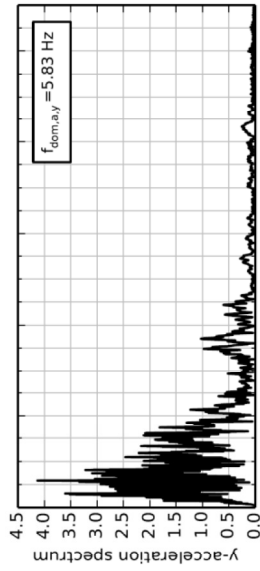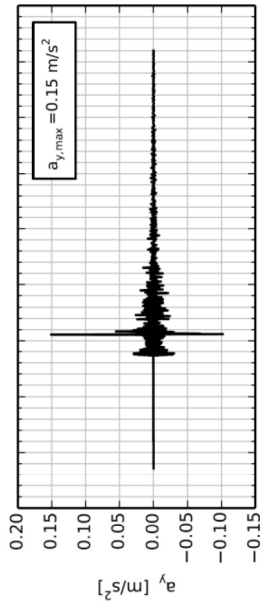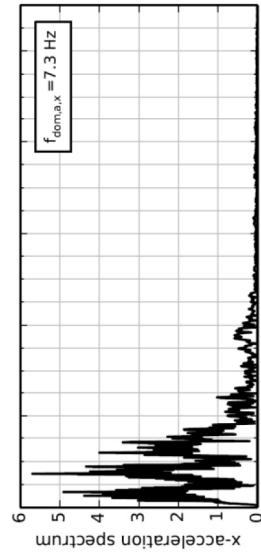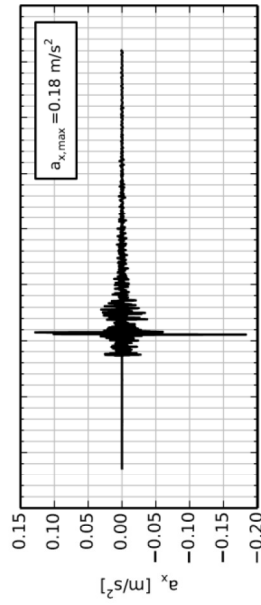
Event Time (UTC): Sep 30 2015 18:05:36.799, TNO ID=629, $|a(t)|_{max} = 0.07 m/s^2$
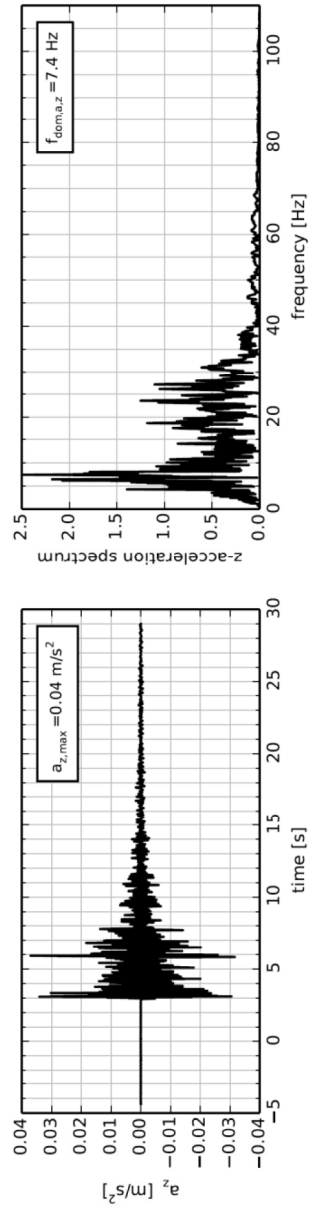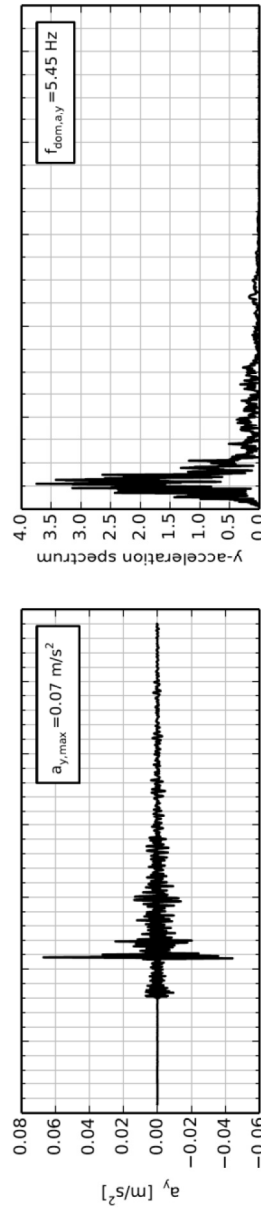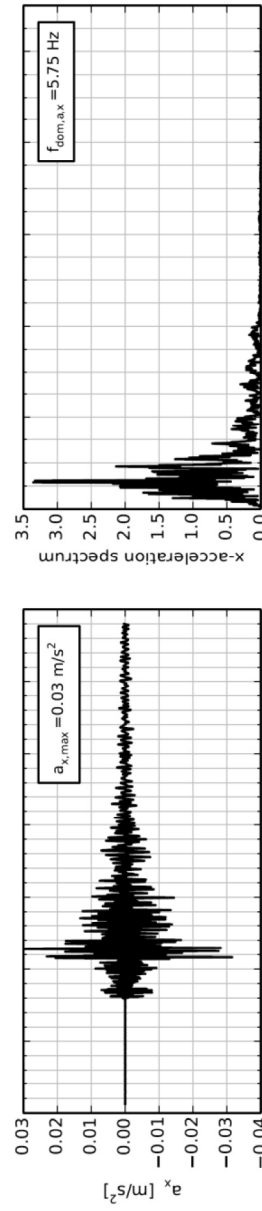
C   Vibration signals – velocity

This Annex gives an example of the vibration velocity signals. For four buildings, with different levels of velocity, the following graphs are given:

- Measured velocity (v_x, v_y, v_z)
- Distribution of the frequency ($f_{dom,v,x}$, $f_{dom,v,y}$, $f_{dom,v,z}$)
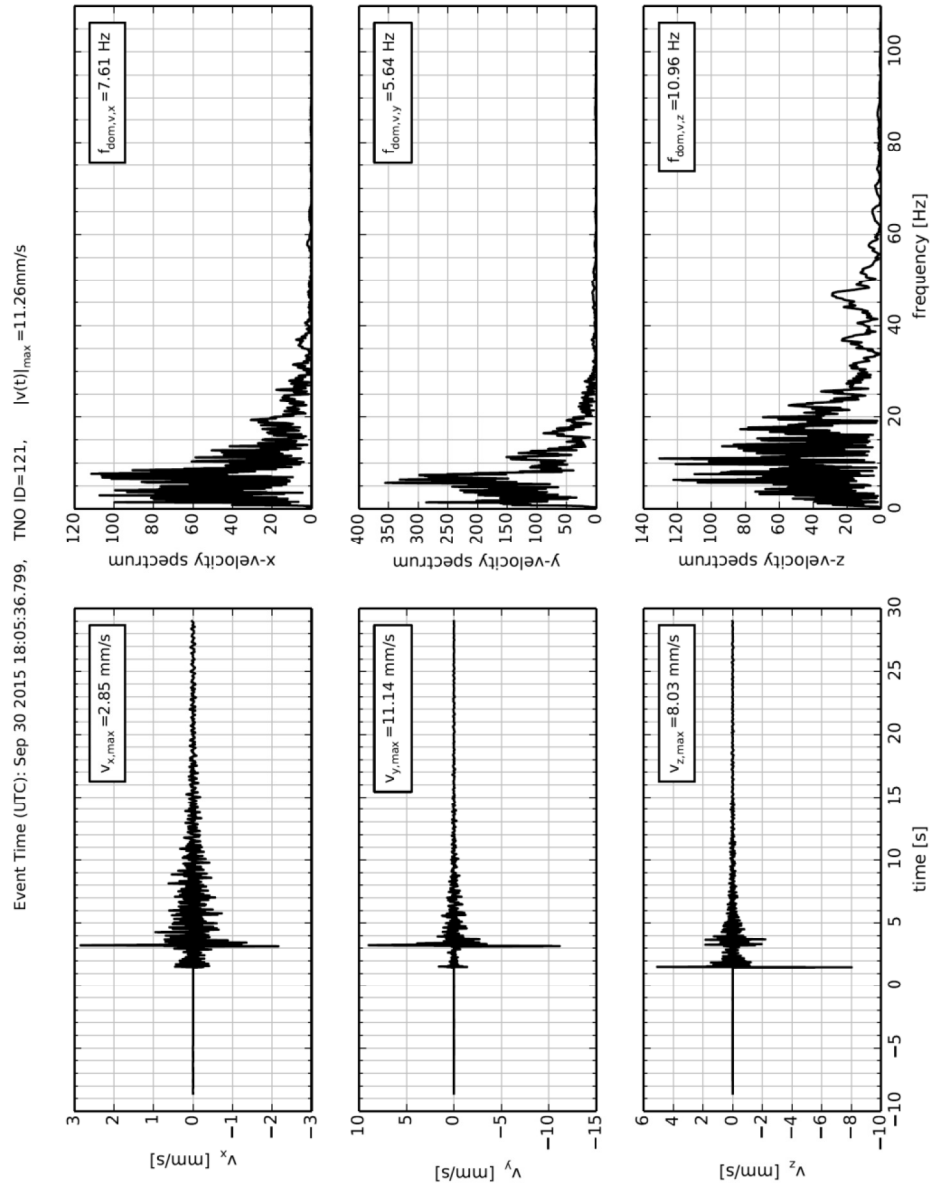
Event Time (UTC): Sep 30 2015 18:05:36.799,   TNO ID=309, $|v(t)|_{max}$ =7.64mm/s
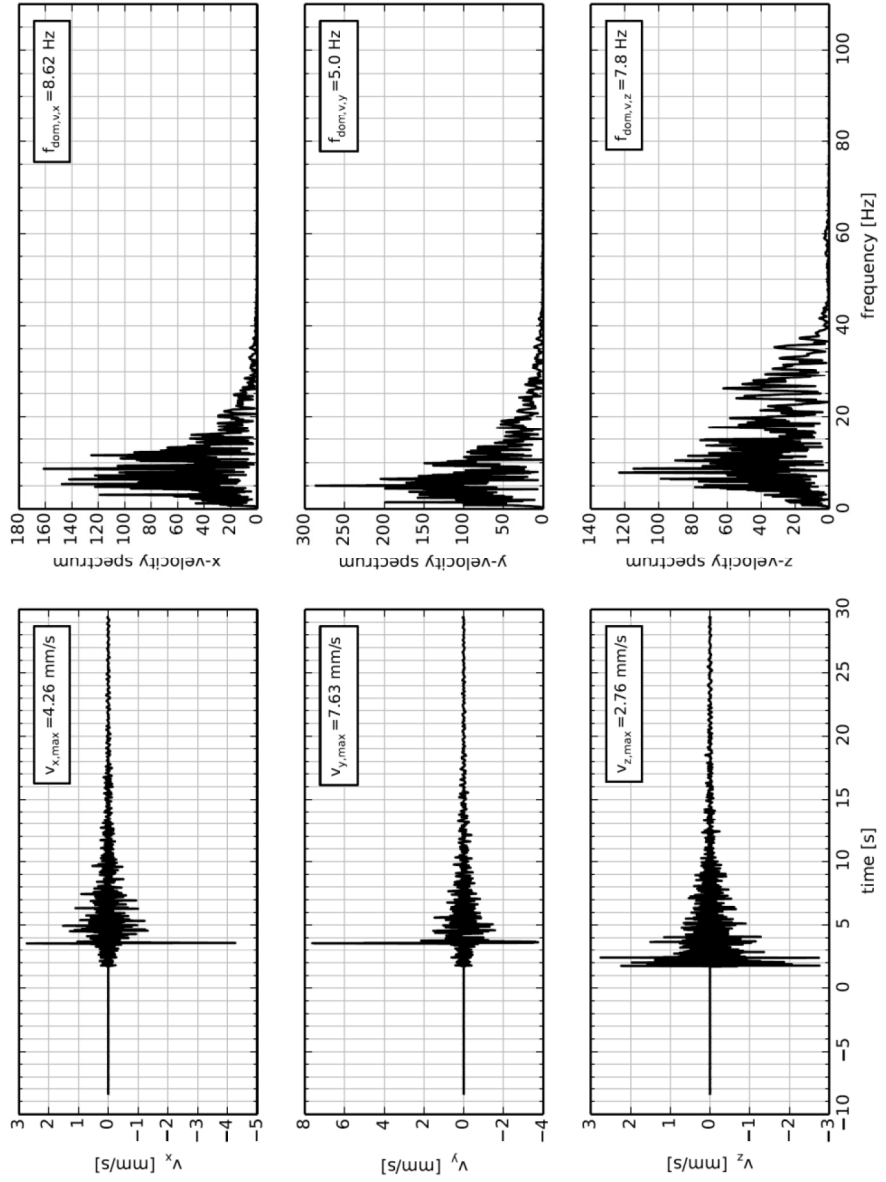
Event Time (UTC): Sep 30 2015 18:05:36.799, TNO ID=36, |v(t)|_max =5.89mm/s
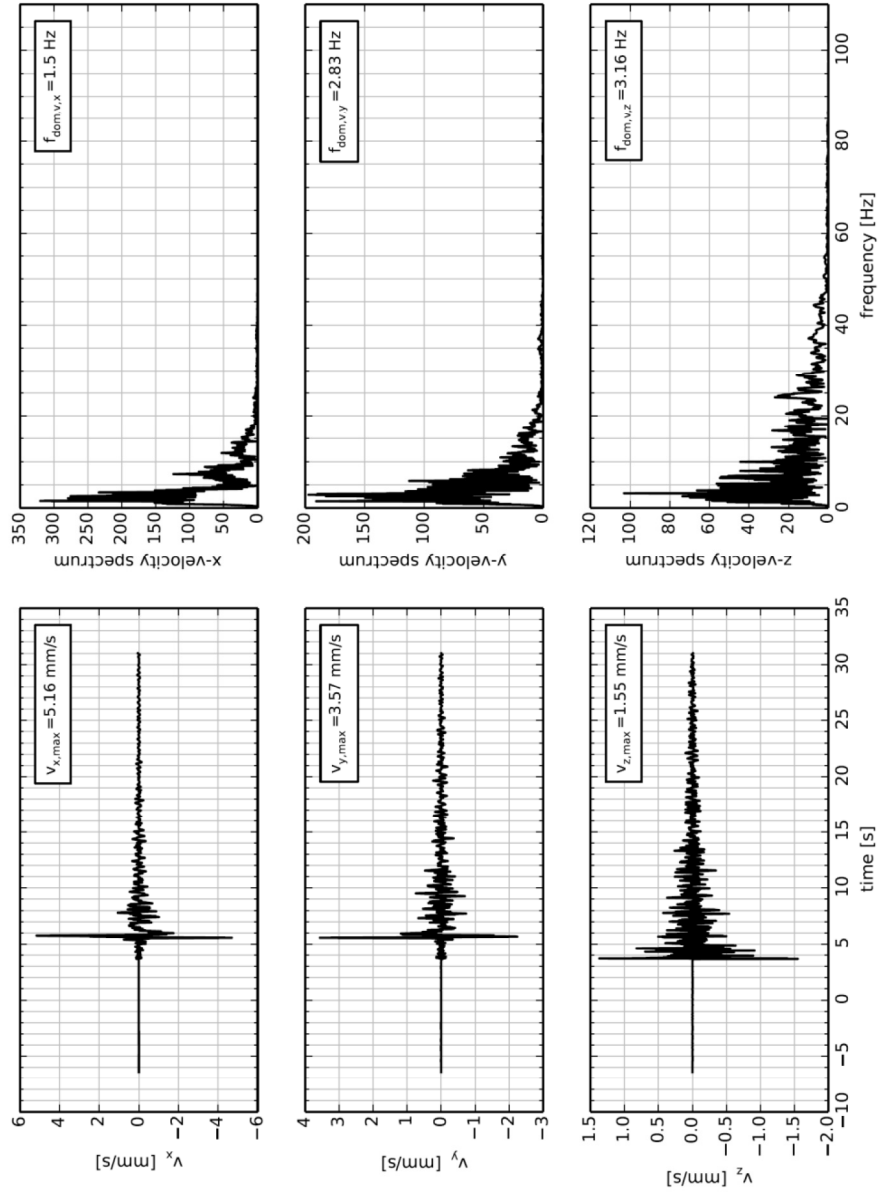
Event Time (UTC): Sep 30 2015 18:05:36.799, TNO ID=629, |v(t)|_max =2.13mm/s
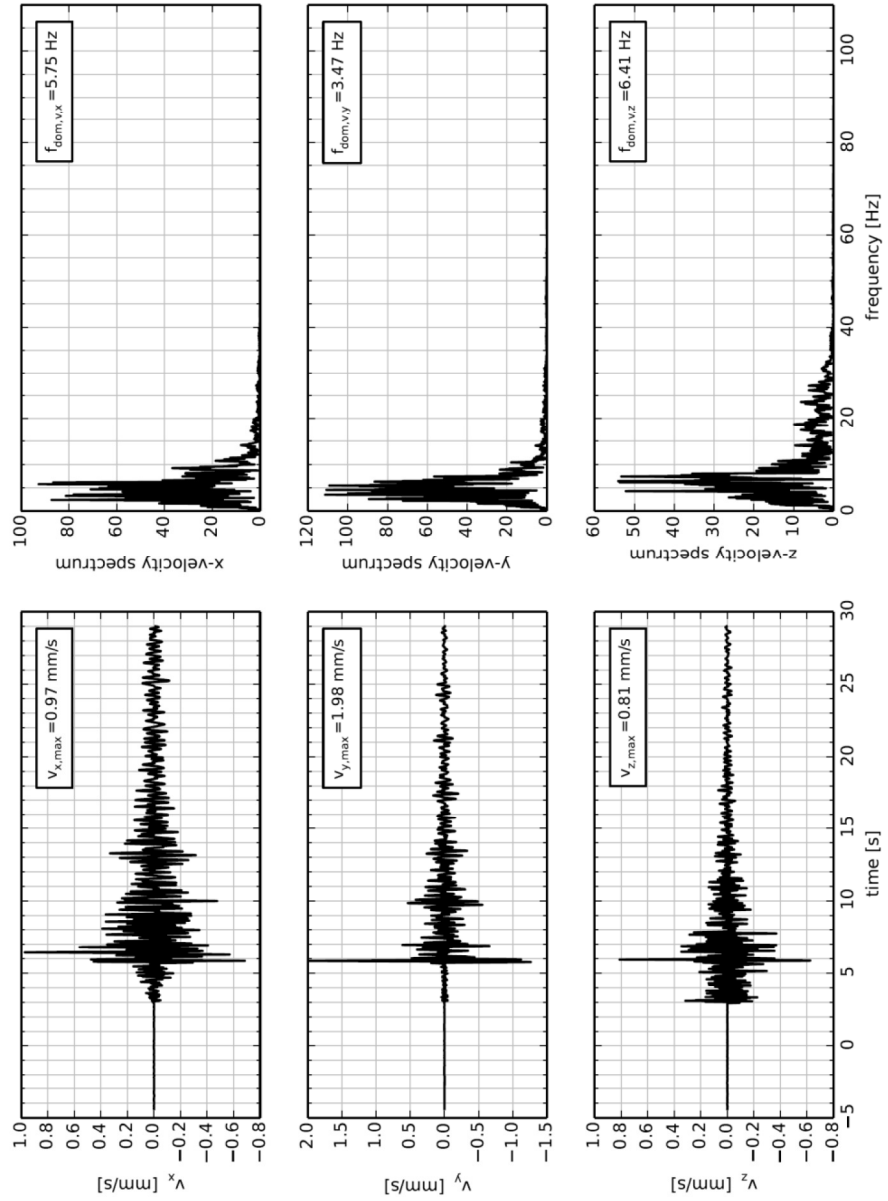
D   Vibration characteristics regarding acceleration

ID	$a_{x,max}$ (m/s²)	$a_{y,max}$ (m/s²)	$a_{z,max}$ (m/s²)	$a_{x,y,max}$ (m/s²)	$|a(t)|_{max}$ (m/s²)	$f_{a,dom,x}$ (Hz)	$f_{a,dom,y}$ (Hz)	$f_{a,dom,z}$ (Hz)
▮	0.16	0.15	0.22	0.16	0.22	11.2	8.2	10.8
▮	0.18	0.15	0.26	0.18	0.26	7.3	5.8	24.1
▮	0.02	0.03	0.01	0.03	0.03	8.3	3.0	10.3
▮	0.26	0.27	0.32	0.27	0.32	4.9	12.3	15.8
▮	0.17	0.17	0.14	0.17	0.22	8.9	4.9	13.8
▮	0.03	0.04	0.06	0.04	0.06	8.3	6.6	100.0
▮	0.25	0.33	0.47	0.33	0.47	8.0	6.3	20.2
▮	0.17	0.65	1.17	0.65	1.17	7.6	7.4	46.9
▮	0.21	0.34	0.50	0.34	0.50	8.7	8.1	20.4
▮	0.05	0.07	0.08	0.07	0.08	7.9	10.4	11.9
▮	0.10	0.19	0.15	0.19	0.20	10.8	10.0	9.3
▮	0.23	0.23	0.60	0.23	0.60	10.1	10.4	19.6
▮	0.06	0.10	0.10	0.10	0.10	7.9	5.6	27.6
▮	0.07	0.04	0.10	0.07	0.10	7.7	6.6	9.7
▮	0.17	0.29	0.34	0.29	0.34	9.0	8.2	12.8
▮	0.34	0.49	0.61	0.49	0.61	9.7	13.1	9.7
▮	0.34	0.51	0.46	0.51	0.52	11.5	9.8	26.1
▮	0.04	0.02	0.01	0.04	0.04	5.3	5.5	9.2
▮	0.05	0.07	0.11	0.07	0.11	6.6	9.2	23.7
▮	0.07	0.05	0.04	0.07	0.07	5.4	8.6	11.4
▮	0.02	0.05	0.03	0.05	0.06	2.4	2.5	106.2
▮	0.05	0.04	0.02	0.05	0.05	6.9	5.9	12.4
▮	0.11	0.18	0.19	0.18	0.21	6.0	2.8	10.9
▮	0.21	0.36	0.19	0.36	0.38	7.7	12.1	16.2
▮	0.36	0.24	0.22	0.36	0.38	12.2	7.7	13.8
▮	0.03	0.04	0.02	0.04	0.04	5.2	5.9	9.0
▮	0.03	0.02	0.02	0.03	0.03	5.9	5.1	8.7
▮	0.05	0.04	0.06	0.05	0.06	9.2	10.6	24.6
▮	0.05	0.07	0.07	0.07	0.08	8.9	8.1	14.8
▮	0.03	0.07	0.04	0.07	0.07	5.7	5.4	7.4
▮	0.04	0.07	0.03	0.07	0.07	8.7	5.0	17.5
▮	0.20	0.20	0.07	0.20	0.24	7.1	50.0	5.3
▮	0.03	0.04	0.02	0.04	0.04	7.3	8.8	3.8
▮	0.05	0.07	0.03	0.07	0.08	7.6	7.5	19.2
▮	0.03	0.03	0.03	0.03	0.04	8.1	4.3	5.2

ID	$a_{x,max}$ (m/s^2)	$a_{y,max}$ (m/s^2)	$a_{z,max}$ (m/s^2)	$a_{x,y,max}$ (m/s^2)	$|a(t)|_{max}$ (m/s^2)	$f_{a,dom,x}$ (Hz)	$f_{a,dom,y}$ (Hz)	$f_{a,dom,z}$ (Hz)
▬	0.03	0.03	0.03	0.03	0.04	6.1	4.4	5.9
▬	0.03	0.02	0.01	0.03	0.03	4.1	4.1	12.6
▬	0.15	0.31	0.37	0.31	0.37	7.8	3.7	18.4
▬	0.04	0.03	0.03	0.04	0.05	4.9	6.1	7.9

E   Vibration characteristics regarding velocity

ID	$v_{x,max}$ (mm/s)	$v_{y,max}$ (mm/s)	$v_{z,max}$ (mm/s)	$v_{x,y,max}$ (mm/s)	$|v(t)|_{max}$ (mm/s)	$f_{v,dom,x}$ (Hz)	$f_{v,dom,y}$ (Hz)	$f_{v,dom,z}$ (Hz)
⬛	2.30	2.64	1.47	2.64	3.42	5.8	8.2	5.9
⬛	5.16	3.57	1.55	5.16	5.89	1.5	2.8	3.2
⬛	0.39	1.02	0.25	1.02	1.02	1.3	3.0	7.4
⬛	3.40	5.04	2.02	5.04	5.20	4.9	7.1	9.0
⬛	3.19	2.45	1.09	3.19	3.85	4.8	4.9	9.3
⬛	0.99	1.13	0.45	1.13	1.29	2.3	6.6	1.6
⬛	3.78	6.83	4.77	6.83	7.50	1.4	1.8	5.3
⬛	2.85	11.14	8.03	11.14	11.26	7.6	5.6	11.0
⬛	3.73	6.88	5.02	6.88	7.61	2.3	1.4	7.5
⬛	1.59	1.55	0.82	1.59	2.19	2.5	2.9	2.8
⬛	2.45	5.21	1.11	5.21	5.54	1.6	2.2	2.9
⬛	5.26	4.16	5.51	5.26	6.69	3.5	1.3	3.8
⬛	1.16	1.99	0.66	1.99	2.01	3.5	5.6	8.5
⬛	1.51	1.07	1.17	1.51	1.60	7.7	4.4	7.2
⬛	2.37	6.75	3.26	6.75	6.75	8.9	1.5	12.8
⬛	5.83	6.22	5.45	6.22	7.80	7.7	3.6	9.7
⬛	4.26	7.63	2.76	7.63	7.64	8.6	5.0	7.8
⬛	1.10	0.54	0.13	1.10	1.12	2.6	2.3	3.1
⬛	1.01	1.57	1.22	1.57	1.57	1.5	2.6	6.1
⬛	1.70	1.10	0.49	1.70	1.86	5.4	5.1	7.8
⬛	0.93	2.00	0.44	2.00	2.04	2.4	2.5	4.2
⬛	1.23	1.49	0.34	1.49	1.50	2.4	5.0	2.4
⬛	2.61	5.05	1.99	5.05	5.60	2.4	2.0	1.8
⬛	2.51	5.32	1.55	5.32	5.45	7.7	2.4	11.1
⬛	5.31	2.64	1.72	5.31	5.40	2.4	7.7	11.4
⬛	0.80	1.19	0.45	1.19	1.23	2.3	3.3	9.0
⬛	1.12	0.69	0.28	1.12	1.13	4.3	2.3	4.5
⬛	1.61	0.86	0.53	1.61	1.65	3.6	3.7	2.5
⬛	1.52	1.92	0.61	1.92	1.93	3.0	2.9	3.8
⬛	0.97	1.98	0.81	1.98	2.13	5.7	3.5	6.4
⬛	0.76	1.53	0.43	1.53	1.56	2.8	2.3	4.3
⬛	4.48	3.83	1.14	4.48	5.51	7.1	5.1	4.1
⬛	0.74	1.31	0.24	1.31	1.43	3.1	3.4	3.8
⬛	1.36	1.62	0.49	1.62	1.83	3.9	3.9	3.4
⬛	1.12	1.17	0.51	1.17	1.56	2.5	2.9	3.3

ID	$v_{x,max}$ (mm/s)	$v_{y,max}$ (mm/s)	$v_{z,max}$ (mm/s)	$v_{x,y,max}$ (mm/s)	$|v(t)|_{max}$ (mm/s)	$f_{v,dom,x}$ (Hz)	$f_{v,dom,y}$ (Hz)	$f_{v,dom,z}$ (Hz)
▬	1.00	0.81	0.52	1.00	1.30	3.3	4.4	3.3
▬	1.00	0.36	0.25	1.00	1.01	2.5	4.1	4.8
▬	4.37	10.26	3.04	10.26	10.40	2.5	2.5	3.8
▬	1.11	0.66	0.29	1.11	1.19	2.5	2.9	1.6

ID	$v_{eff,x,max}$ (mm/s)	$v_{eff,y,max}$ (mm/s)	$v_{eff,z,max}$ (mm/s)	$v_{eff,max}$ (mm/s)
▬	0.93	0.97	0.59	0.97
▬	1.49	1.12	0.64	1.49
▬	0.17	0.31	0.11	0.31
▬	1.44	1.70	0.82	1.70
▬	1.13	1.11	0.49	1.13
▬	0.31	0.46	0.21	0.46
▬	1.48	2.14	1.47	2.14
▬	0.99	4.19	2.24	4.19
▬	1.31	2.13	1.53	2.13
▬	0.57	0.53	0.36	0.57
▬	0.90	1.65	0.48	1.65
▬	1.94	1.79	1.73	1.94
▬	0.45	0.69	0.30	0.69
▬	0.56	0.41	0.46	0.56
▬	0.96	2.20	1.30	2.20
▬	2.34	2.34	1.56	2.34
▬	1.56	2.48	1.13	2.48
▬	0.42	0.21	0.07	0.42
▬	0.35	0.58	0.51	0.58
▬	0.55	0.37	0.25	0.55
▬	0.29	0.65	0.22	0.65
▬	0.45	0.59	0.13	0.59
▬	0.79	1.64	0.69	1.64
▬	1.01	1.65	0.58	1.65
▬	1.66	1.02	0.55	1.66
▬	0.29	0.48	0.20	0.48
▬	0.45	0.27	0.11	0.45
▬	0.54	0.27	0.22	0.54
▬	0.47	0.66	0.27	0.66
▬	0.34	0.75	0.33	0.75
▬	0.36	0.62	0.19	0.62

ID	$v_{eff,x,max}$ (mm/s)	$v_{eff,y,max}$ (mm/s)	$v_{eff,z,max}$ (mm/s)	$v_{eff,max}$ (mm/s)
■	1.86	1.59	0.41	1.86
■	0.29	0.45	0.10	0.45
■	0.56	0.67	0.18	0.67
■	0.36	0.37	0.21	0.37
■	0.33	0.26	0.22	0.33
■	0.29	0.16	0.10	0.29
■	1.30	3.30	1.23	3.30
■	0.39	0.28	0.09	0.39

F Vibration characteristics regarding Cumulative Absolute Velocity (CAV)

TNO ID	CAV_x [mm/s]	CAV_y [mm/s]	CAV_z [mm/s]	CAV_{total} [mm/s]	$CAV_{STD,X}$ [mm/s]	$CAV_{STD,y}$ [mm/s]	$CAV_{STD,z}$ [mm/s]	$CAV_{STD,TOTAL}$ [mm/s]
■	100.0	126.3	127.5	353.8	84.1	113.0	109.3	306.5
■	92.5	82.6	93.2	268.4	67.6	59.7	68.8	196.2
■	23.9	28.5	20.0	72.3	4.6	6.8	3.9	15.3
■	145.6	171.3	179.1	495.9	131.5	150.5	161.3	443.2
■	115.9	90.5	118.4	324.8	96.2	74.3	106.0	276.4
■	83.9	96.6	61.9	242.5	62.4	76.4	34.5	173.2
■	100.0	132.9	117.5	350.5	80.7	113.5	99.1	293.3
■	136.3	213.6	200.4	550.2	118.6	193.3	180.1	492.0
■	83.4	114.7	124.8	322.9	61.0	98.5	107.8	267.3
■	94.2	98.4	73.5	266.1	73.6	76.6	51.9	202.2
■	96.4	127.1	101.3	324.8	77.7	107.2	77.7	262.6
■	116.9	108.3	122.5	347.7	97.7	91.1	100.3	289.1
■	48.6	71.9	69.0	189.6	18.1	50.1	52.0	120.2
■	68.2	76.8	73.9	219.0	43.1	52.8	51.3	147.3
■	131.1	159.0	171.4	461.4	111.9	142.6	159.6	414.1
■	146.8	160.2	175.9	482.8	128.6	141.8	153.8	424.2
■	170.1	206.3	231.5	607.9	148.1	188.3	212.6	549.0
■	35.2	29.7	17.4	82.3	12.2	13.6	0.0	25.8
■	59.3	50.3	61.3	170.9	42.7	27.1	48.0	117.8
■	54.8	46.8	58.6	160.2	35.7	22.1	48.4	106.2
■	62.6	60.5	34.7	157.8	36.3	26.2	18.5	80.9
■	54.1	61.7	42.8	158.6	32.1	41.7	19.9	93.7
■	75.2	103.0	91.2	269.3	53.9	85.0	73.0	211.8
■	96.0	131.1	126.1	353.1	77.3	119.1	108.4	304.8
■	125.8	107.4	144.5	377.8	110.6	89.7	128.3	328.6
■	51.6	66.0	54.5	172.1	27.7	40.2	33.9	101.8
■	56.6	49.6	39.6	145.7	28.3	23.8	18.8	70.8
■	83.2	88.5	77.0	248.6	59.1	66.6	58.3	184.1
■	86.8	86.5	78.4	251.8	64.8	61.1	55.4	181.3
■	58.6	57.7	48.4	164.7	31.1	29.0	33.6	93.7
■	63.9	65.2	47.8	176.8	40.9	42.3	29.0	112.3
■	149.7	171.2	101.2	422.1	124.8	118.4	75.8	319.1
■	51.1	60.0	35.9	147.0	22.3	29.3	7.4	59.1

TNO ID	CAV$_x$ [mm/s]	CAV$_y$ [mm/s]	CAV$_z$ [mm/s]	CAV$_{total}$ [mm/s]	CAV$_{STD,X}$ [mm/s]	CAV$_{STD,y}$ [mm/s]	CAV$_{STD,z}$ [mm/s]	CAV$_{STD,TOTAL}$ [mm/s]
■	63.1	69.6	59.7	192.4	39.4	48.3	36.3	124.0
■	53.4	54.6	50.0	158.1	29.5	30.8	25.7	86.0
■	64.7	67.7	50.9	183.3	37.6	44.5	30.4	112.4
■	23.7	23.0	28.2	75.0	8.2	6.9	14.1	29.2
■	139.8	211.5	148.3	499.6	118.3	183.0	126.0	427.4
■	48.9	43.3	23.3	115.4	14.4	20.4	1.1	35.9

G   Vibration characteristics Arias Intensity (I_A)

TNO ID	$I_{A,X}$ [mm/s]	$I_{A,Y}$ [mm/s]	$I_{A,Z}$ [mm/s]	$I_{A,TOTAL}$ [mm/s]
▬	0.36	0.59	0.66	1.61
▬	0.42	0.24	0.52	1.18
▬	0.01	0.02	0.01	0.04
▬	0.84	1.19	1.35	3.38
▬	0.51	0.31	0.53	1.36
▬	0.10	0.16	0.08	0.34
▬	0.52	1.08	1.43	3.03
▬	0.60	3.89	4.79	9.28
▬	0.37	0.92	1.76	3.06
▬	0.18	0.21	0.13	0.52
▬	0.27	0.76	0.36	1.40
▬	0.67	0.67	1.63	2.96
▬	0.07	0.15	0.24	0.46
▬	0.11	0.11	0.19	0.41
▬	0.61	1.34	1.97	3.92
▬	1.28	1.77	2.67	5.71
▬	1.06	2.06	2.96	6.08
▬	0.03	0.02	0.01	0.06
▬	0.09	0.09	0.20	0.38
▬	0.10	0.07	0.10	0.26
▬	0.06	0.08	0.03	0.17
▬	0.06	0.10	0.03	0.19
▬	0.19	0.49	0.44	1.13
▬	0.38	1.07	0.68	2.13
▬	1.05	0.50	0.90	2.45
▬	0.05	0.08	0.05	0.18
▬	0.06	0.04	0.03	0.13
▬	0.12	0.13	0.13	0.37
▬	0.15	0.20	0.16	0.50
▬	0.07	0.10	0.06	0.23
▬	0.09	0.11	0.05	0.25
▬	0.82	0.61	0.27	1.70
▬	0.04	0.07	0.02	0.13

TNO ID	$I_{A,X}$ [mm/s]	$I_{A,Y}$ [mm/s]	$I_{A,Z}$ [mm/s]	$I_{A,TOTAL}$ [mm/s]
██	0.11	0.14	0.07	0.32
██	0.05	0.06	0.05	0.15
██	0.07	0.08	0.05	0.20
██	0.01	0.01	0.02	0.04
██	0.50	1.95	1.42	3.86
██	0.05	0.04	0.01	0.10

H   Registration form for repetitive damage survey

Tabel voor herhalingsopname n.a.v. aardbeving

Id - Postcode	
Naam	
Adres	
Woonplaats	

Volgnummer herhalingsopname	
Datum herhalingsopname	

Aardbeving	Locatie en datum	Vmax		mm/s
	Locatie en datum	Vmax		mm/s
	Locatie en datum	Vmax		mm/s

Gevel	Scheurnr.	Locatie	Scheurwijdte A=<1mm; B=1-10mm; C=>10mm	Foto scheur	W(ijder) / L(anger) / H(ersteld) / O(nveranderd)	Nieuwe scheurwijdte	Foto scheur
Bestaande scheuren							
Nieuwe scheuren							
Opmerkingen							

I Results repetitive damage survey

ID	previous damage survey			Repetitive damage survey				
	Amount of cracks			Amount of cracks increased		Amount of new cracks		
	Cat.A	Cat.B	Cat.C	In same category	In higher category	Cat.A	Cat.B	Cat.C
■	8	12	0	0	0	6	0	0
■	1	0	0	0	0	0	0	0
■	2	0	0	0	0	1	0	0
■	2	2	0	0	0	8	0	0
■	2	0	0	0	0	7	1	0
■	36	1	0	0	0	0	0	0
■	5	0	0	0	0	0	0	0
■	3	0	0	0	0	1	0	0
■	4	5	2	0	0	1	0	0
■	4	3	0	0	0	15	5	0
■	10	0	0	0	0	4	0	0
■	41	15	0	0	0	1	0	0
■	7	0	0	0	0	0	0	0
■	2	0	0	0	0	1	1	0
■	6	4	0	1	0	4	0	0
■	3	0	0	0	0	0	0	0
■	7	0	0	0	0	0	0	0
■	6	0	0	0	0	0	0	0
■	1	1	0	0	0	11	5	0
■	2	0	0	0	0	0	0	0
■	14	4	0	0	0	0	0	0
■	3	1	0	0	0	0	0	0
■	1	1	0	0	0	1	1	0
■	1	0	0	0	0	1	0	0
■	10	0	0	0	0	0	0	0
■	1	0	0	1	0	1	0	0
■	15	0	0	0	0	1	0	0
■	4	14	5	0	0	2	0	0
■	0	0	0	0	0	1	0	0
■	9	2	0	0	0	2	0	0
■	7	1	0	0	0	0	0	0
■	6	0	0	0	0	0	0	0
■	13	3	0	0	0	0	0	0
■	3	0	0	0	0	2	0	0
■	2	3	0	0	0	3	0	0
■	55	4	0	0	2	0	0	0
■	5	0	0	0	0	3	0	0
Total	301	76	7	2	2	77	13	0

ID	Remarks
▬	Two cracks already visible on photos of previous survey
▬	A few new cracks are present in repair works, executed before the initial survey
▬	Seven cracks already visible on photos of previous survey
▬	One crack already visible on photos of previous survey
▬	One crack already visible on photos of previous survey
▬	New crack already visible on photos of previous survey
▬	One crack already visible on photos of previous survey
▬	New crack already visible on photos of previous survey
▬	One crack already visible on photos of previous survey